Response to the Anonymous Referee #2 on the revised version of "Enhanced growth rate of atmospheric particles from sulfuric acid"

Response to Anonymous Referee #2:

The paper has been improved and indeed more information on the experiment and the analysis can now be discerned. There are some crucial issues in the main result that appear to be open to alternate analyses. The change in the approach now taken by the authors is good but the use of dry GR introduces digressions and considerable confusion to this reviewer. Below I calculate and report a 'wet' GR that the particles actually undergo in the experiment. This alternate analysis suggests the enhancement in collisional rates due to van der Waals forces is less than their analysis suggests. The authors' discussion of the issues raised in (1) and (2) will illuminate the best way forward.

We are thankful to the reviewer for the careful analysis of our updated calculations. We feel that an even more thorough discussion of the effects of water will improve this manuscript. The main change in the revised manuscript is to compare three approaches describing hygroscopicity and to revise Figure 4b. As the figure shows, these three very different approaches to treating the effects of water have little quantitative and negligible qualitative effect on our conclusions. We therefore argue that our conclusions are robust. We also agree with the reviewer that several aspects still need to be clarified and thus we re-organized the manuscript by including large parts from the Supplement into a Methods section in order to ensure all key information is present in the main text. We also updated all Figures to have a more publication-ready format and hope this improves the presentation quality.

(1) The explicit inclusion of the particle's water content in the analysis is quite important for growth rates and the derived collision rate coefficients. Yet there is only a modest change in the results! Inspection of the previous eqn (S1) revealed that a factor of two was used to "include collisions in both ways". This factor was not justified in the first version (thanks to Chris Hogan's close look) and now the authors have dropped it, claiming that another factor of two canceled it. Can the authors explain the evolution of their thought in developing eqn (S1)? Where did the"collisions in both ways" idea come from? It seems that previously they used the kcoll from Niemenen et al. It is not clear how the factor of two was canceled out in the last version and what is going on with the revised calculations.

In the answer to Chris Hogan's comment, we showed the origin of the error (taking the kernels from Chan & Mozurkewich 2001), and the reason why the factor did cancel already in the first place (a factor of 2 used in front of the collision kernel). This is well summarized in the public response to Chris Hogan. We corrected the equations, deleted the sentence of the "collision in both ways" and updated the calculations. We also modified the entire theory section of the growth rate derivation to give it a more logical structure in the revised version. Thus we are confident that the reader of the revised manuscript will understand how the calculations have been performed.

(1b) The assumption that the dry volume of the gaseous H2SO4 molecules can be assigned to the change in the dry volume of the particles has not been shown to be true. Furthermore, H2SO4 hydration is a matter of wide variability according to the quantum chemistry studies; why choose Henschel over Temelso and how much of an effect does an alternate choice make?

(2) The growth factor expression seems a bit odd and needs a reference. It seems a more standard expression would have in the numerator the density times weight fraction w of the appropriate RH in the instrument. Looking at the data for 5 nm dry mass diameter, the numerator has a value of 1.68 to get the gf in the figure. This is the density of 76 wt % SA. Applying this w to the numerator, gf is 1.24 for a dry mass diameter of 5 nm.

(3) Using the data in Figures S1(b,c, [SA]=2.1e7 cm-3) and applying gf of 1.2 and 1.28 for the 2.9 and 7.7 mass diameter, one gets an experimental GR of 3.2 nm/hr over the 3.2 to 8 nm dry mob. diameter range. Compare this value to the GR calculated using the 'wet' GR from eqn. (7) of Verheggen and Mozurkewich (JGR, 2002), one gets a GR of 2.17 nm/hr for 48 wt. % SA (the SA-content for the midrange dry mass diameter of 5 nm): 1.95 nm/hr from the first term on the RHS, involving growth by SA uptake, and 0.22 nm/hr for the 2nd term, particle swelling due to the change in composition with size. Incorporating the size of the condensing molecule into eqn (7) of Verh. and Moz. (2002), by applying a factor of (1+dv/dp)2 to the first term and the total GR is 2.6 nm/hr, about 20 % less than the experimental GR. This analysis has a hardsphere GR that departs from experimental somewhat less than what appears to be in the paper.

These three points help to clarify the effect of water on our measured growth rates. The reviewer is correct that the assumptions of dry particles at 5 % RH is questionable and that the numerator in Eq. (13) of the revised manuscript needs to be defined differently (the numerator needs to include the mass fraction of the measurement, see e.g. Biskos et al., 2009, J. Aerosol Sci.). We also appreciate the reviewer pointing us towards the paper of Verheggen and Mozurkewich (2002), which offers a different view on the problem. As also pointed out by the reviewer, composition data are important if we follow this approach. This is true for both chamber and measurement conditions. We hence decided to compare three approaches in the revised manuscript and discuss their agreement with the measurement data in an entirely new section in the revised manuscript.

A first naïve approach which follows the first version of the manuscript, i.e. taking an average hydration of the monomer and assuming this to be the same for the growing particle, which is unaltered during the measurement. Here it is important to note that the results from Temelso 2012, Henschel 2014, Kurten 2007 and Wexler and Clegg 2002 actually agree quite well, all predicting an average hydration of either 1 or 2 H_2O molecules at around 50% RH. Overall, for the conditions of our measurements, we do not find the variety of hydration results in the recent literature, contrary to the assertion of the reviewer. Most probable hydration is either 1 or 2 water molecules per sulfuric acid under our experimental conditions and this is covered in our uncertainty estimate already.

Second, we adjusted the naïve measurement approach, by acknowledging the fact that the actual particle size is measured dry. For this we assume a hygroscopic growth factor of 1.25, which is the average value of the results of Biskos et al. (2009), J. Aerosol Sci., for sub-10 nm particles at 40-60% RH. All HTDMA studies, which have served as a basis for composition data, base their measured growth factors also from a dry size at or around 5 % RH, i.e. close to the conditions of the DMA-train, which allows us to choose such a value from literature. The reviewer is correct that the mass addition per collision to a particle at 5% RH might still be influenced by water, but composition data for 5% RH is basically not available from measurements, but only from models. Here, e.g. MABNAG predicts almost no hydration at 5 % RH for particles larger than 3 nm, so the assumption of a dry measurement does not seem to be a huge oversimplification.

Third, we followed the approach of Verheggen & Mozurkewich (2002) and used both SAWNUC and MABNAG to both predict hydration of particles in the chamber and during the measurement. In this approach the effect of water uptake and sulfuric acid driven growth are separated (thus called separation approach in our revised manuscript). All three approaches yield similar results for the collision enhancement (and the Hamaker constant), if we use the MABNAG composition data. We show a comparison of the approaches with the measured growth rates in Fig. 4b of the revised manuscript. We also show the results when using SAWNUC for the separation approach, which do not agree well with our measurements. While SAWNUC certainly estimates the hydration of the smaller clusters better than MABNAG (which was already identified in Yli-Juuti et al., 2013, ACP), SAWNUC might predict a too low sulphuric acid mass fraction at larger sizes. This could be mainly due to the effect that even at the low ammonia levels of the measurements, neutralization occurs to some extend as predicted by MABNAG. Hence, we come to the conclusion that the constant growth factor assumed in the dry measurement approach might give a good estimate at small and larger sizes and that additional swelling by water might be a minor effect.

Altogether, all three approaches yield a Hamaker constant which is well within our overall systematic uncertainty estimate (note that all of them are within the uncertainty estimate of the first version of this paper). We therefore come to the final conclusion that, independent of the approach, the Hamaker constant can be well estimated by our final given value and uncertainty range of $A = 5.2^{+9.7}_{-3.4}(syst.) \cdot 10^{-20}$J.

(4) Composition data is incredibly important here and Fig. S4a is a welcome figure. Yet the composition etc. inside the instrument is also needed (the numerator in the gf eqn). Having said that, the Fig. S4a SAWNUC composition data has not really been put to any stringent tests: it was the nucleation rates - for cold conditions - that were verified in Ehrhart et al. 2016 (or have I missed something in that work?) Variations in rho and w should be considered in the uncertainty analysis. Also important in this is that ammonia was present which is not considered in SAWNUC, thus more uncertainty.

The reviewer is correct that the assumed composition data from SAWNUC might be one of the weaknesses in this approach and that they were verified with data from 278 K downwards. Especially SAWNUC does not include ammonia, which could cause some neutralization of the small particles even at concentrations as low as 3 pptv. We therefore also present the predicted the particle hydration by calculations with MABNAG in the revised manuscript.

Variations in w (and hence in rho) were already considered in the last version of the manuscript. Nevertheless, they are again included and discussed in our updated Figure S5 in the Supplement.

(5) As to the data for growth between 1.8 and 3.2 nm mobility diameter. The 1.8 nm data does not show fidelity to the assumed time dependence as there is a slow climb in the count rate over the hours (Fig. S1). What is the physical reason for the assumed shape of the appearance curve (a systematic concern)? Also, the composition of the 'dried' 1.8 nm particles would be most affected by charge, even the SAWNUC calculations allude to that (Ehrhart (2016) plot). Ammonia might affect the smallest channels differently than it would the larger channels. Aside from systematic biases, there is a significant random uncertainty in the appearance time for the small diameter channels, many (5 or 10?) minutes. To better serve the reader, there needs to be two paragraphs added to the main text. (i) An experimental paragraph on how the DMA's were deployed and the experimental conditions in them (e.g., 5 % RH is due to dry sheath gas diluting the incoming moist sample aerosol? Change in temperature upon sampling? Sampling arrangement?) (ii) A paragraph describing the main assumptions in the appearance time method, e.g. answering the questions raised above.

We respectfully disagree with the reviewer. First, we do not see any significant climb in count rate over the hours in Figure S1. There are some small fluctuations which might come from fluctuations in the nucleation rate (see also the slowly increasing trend of ammonia over the same time-span) and these are also visible in the other size channels. The appearance time fit however is chosen to cover a similar time-range for all channels, making the linear fit robust. Hence, we are highly confident that the agreement between the appearance time fit and the measured data is sufficient to provide a good growth rate measurement. The appearance time method is well-documented in literature and hence we

do not see the need the elaborate in detail on this but refer to a recent published article in Nature Protocols (Dada et al., Nat. Protoc., 2020) in the Methods Section. Second, in our opinion, the effect of charge on the hydration at 1.8 nm is not significant in the Ehrhart et al. (2016) plot (the effect of charge vanishes above 1.5 nm). Moreover, the reported growth rates are integrated growth rates from 1.8-3.2 nm and a close-to-insignificant effect at 1.8 nm would hardly bias the entire growth rate result, which we clarified by stating that the measured growth rates are integrated growth rate from 1.8-3.2 nm in the revised Methods Section. However, the reviewer is correct that the assumed time dependence in the appearance time method fits has no physical basis, which we added in the Methods Section. Certainly, the appearance time method does suffer from systematic uncertainties, and hence we included the calculations using INSIDE. Here the approach is entirely different and the excellent agreement between both methods gives us the high confidence on our dataset. We also agree with the reviewer that we should specify the measurement methods in more detail with respect to the open questions about hydration and we have updated the Methods Section accordingly.

(6) A paragraph in the Supplement describing the Inside method is needed. For example, how do values appear continuously and even at lower diameter then the measurements it is derived from? Why was the TREND method not selected? Pichelstorfer et al. notes that this method is good for capturing the leading edge of growing aerosol. There is also a log normal method. It is notable that there seems to be only partial agreement between these methods when comparing to experimental data.

As the reviewer suggested, we extended our description on the INSIDE method in the Supplement. TREND and INSIDE agree nicely in the size range where both methods yield results. However, INSIDE is evaluated at the same diameters over a larger size range compared to TREND, we used INSIDE to average over an entire run. Note, that also no INSIDE results are reported below 1.8 nm (mobility diameter), so we do not share reviewer's concerns on this. For the problems of the applicability of the lognormal method to chamber data we refer the reviewer to Dada et al. (Nat. Protoc. 2020, p.11): "(…), including the log-normal distribution function method (which is not covered in this protocol because it is often unsuitable for chamber experiments, being that there are no distinct particle modes)".

(7) It is not clear how S9 (previously S6) was obtained nor what the authors mean in the different nomenclature between the terms on the LHS of eqns. S1 and S9. Is one of them an average GR?

This has been clarified in the revised theoretical growth rate section of the revised manuscript.

Enhanced growth rate of atmospheric particles from sulphuric acid

Dominik Stolzenburg[1,2], Mario Simon[3], Ananth Ranjithkumar[4], Andreas Kürten[3], Katrianne Lehtipalo[2,5], Hamish Gordon[4], Sebastian Ehrhart[6], Henning Finkenzeller[7], Lukas Pichelstorfer[2], Tuomo Nieminen[2], Xu-Cheng He[2], Sophia Brilke[1], Mao Xiao[8], António Amorim[9], Rima Baalbaki[2], Andrea Baccarini[8], Lisa Beck[2], Steffen Bräkling[10], Lucía Caudillo Murillo[3], Dexian Chen[11], Biwu Chu[2], Lubna Dada[2], António Dias[9], Josef Dommen[8], Jonathan Duplissy[2], Imad El Haddad[8], ~~Henning Finkenzeller[11]~~, Lukas Fischer[12], Loic Gonzalez Carracedo[1], Martin Heinritzi[3], Changhyuk Kim[13,14], Theodore K. Koenig[7], Weimeng Kong[13], Houssni Lamkaddam[8], Chuan Ping Lee[8], Markus Leiminger[12,15], Zijun Li[16], Vladimir Makhmutov[17], Hanna E. Manninen[18], Guillaume Marie[3], Ruby Marten[8], Tatjana Müller[3], Wei Nie[19], Eva Partoll[12], Tuukka Petäjä[2], Joschka Pfeifer[18], Maxim Philippov[17], Matti P. Rissanen[2,20], Birte Rörup[2], Siegfried Schobesberger[16], Simone Schuchmann[18], Jiali Shen[2], Mikko Sipilä[2], Gerhard Steiner[12], Yuri Stozhkov[17], Christian Tauber[1], Yee Jun Tham[2], António Tomé[21], Miguel Vazquez-Pufleau[1], Andrea C. Wagner[3,7], Mingyi Wang[11], Yonghong Wang[2], Stefan K. Weber[18], Daniela Wimmer[1,2], Peter J. Wlasits[1], Yusheng Wu[2], Qing Ye[11], Marcel Zauner-Wieczorek[3], Urs Baltensperger[8], Kenneth S. Carslaw[4], Joachim Curtius[3], Neil M. Donahue[11], Richard C. Flagan[13], Armin Hansel[12,15], Markku Kulmala[2], Jos Lelieveld[6], Rainer Volkamer[7], Jasper Kirkby[3,18] and Paul M. Winkler[1]

[1]Faculty of Physics, University of Vienna, 1090 Vienna, Austria.
[2]Institute for Atmospheric and Earth System Research/Physics, University of Helsinki, 00014 Helsinki, Finland.

[3]Institute for Atmospheric and Environmental Sciences, Goethe University Frankfurt, 60438 Frankfurt am Main, Germany.
[4]School of Earth and Environment, University of Leeds, Leeds LS2 9JT, United Kingdom.
[5]Finnish Meteorological Institute, 00560 Helsinki, Finland.
[6]Atmospheric Chemistry Department, Max-Planck-Institute for Chemistry, 55128 Mainz, Germany
[7]Department of Chemistry and Cooperative Institute for Research in Environmental Sciences, University of Colorado Boulder, 80309 Boulder CO, USA.
[8]Laboratory of Atmospheric Chemistry, Paul Scherrer Institute, 5232 Villigen, Switzerland.
[9]Center for Astrophysics and Gravitation, Faculty of Sciences of the University of Lisbon, 1749-016 Lisbon, Portugal.
[10]Tofwerk AG, 3600 Thun, Switzerland.
[11]Center for Atmospheric Particle Studies, Carnegie Mellon University, 15217 Pittsburgh PA, USA.
[12]Institute for Ion Physics and Applied Physics, University of Innsbruck, 6020 Innsbruck, Austria.
[13]Division of Chemistry and Chemical Engineering, California Institute of Technology, 91125 Pasadena CA, USA.
[14]Department of Environmental Engineering, Pusan National University, Busan 46241, Republic of Korea.
[15]Ionicon Analytik GmbH, 6020 Innsbruck, Austria.
[16]Department of Applied Physics, University of Eastern Finland, 70211 Kuopio, Finland.
[17]P.N. Lebedev Physical Institute of the Russian Academy of Sciences, 119991 Moscow, Russia.
[18]CERN, the European Organization for Nuclear Research, 1211 Geneva, Switzerland.
[19]Joint International Research Laboratory of Atmospheric and Earth System Sciences, School of Atmospheric Sciences, Nanjing University, 210023 Nanjing, China.
[20]Aerosol Physics Laboratory, Tampere University, 33101 Tampere, Finland.
[21]Institute Infante Dom Luíz, University of Beira Interior, 6200-001 Covilhã, Portugal.

Correspondence to: Paul M. Winkler (paul.winkler@univie.ac.at)

Abstract. In the present-day atmosphere, sulphuric acid is the most important vapour for aerosol particle formation and initial growth. However, the growth rates of nanoparticles (<10 nm) from sulphuric acid ~~vapour~~ remain poorly measured. Therefore, the effect of stabilizing bases, the contribution of ions and the impact of attractive forces on molecular collisions are under debate. Here we present precise growth-rate measurements of uncharged sulphuric acid particles ~~in the size range~~ from 1.8-10 nm, performed under atmospheric conditions in the CERN CLOUD chamber. Our results show that the evaporation of sulphuric acid particles above 2 nm is ~~indeed~~ negligible and growth proceeds kinetically even at low ammonia concentrations. The experimental growth rates exceed the ~~geometric~~ hard-sphere kinetic limit for condensation of sulphuric acid. We demonstrate that this results from van-der-Waals forces between the vapour molecules and particles and disentangle it from charge-dipole interactions. The magnitude of the enhancement depends on the assumed particle hydration and collision kinetics, but is increasingly important at smaller sizes resulting in a steep rise of observed growth rates with decreasing size. ~~, and reveal an enhancement resulting from van der Waals forces between the vapour molecules and particles. We are able to disentangle the effects of charge-dipole interactions and van der Waals forces and observe a steep increase of particle growth rates with decreasing size.~~ Including the experimental results in a global model, we find the enhanced growth rate of sulphuric acid particles increases predicted particle number concentrations in the upper free troposphere by more than 50%.

1 Introduction

Sulphuric acid (H_2SO_4) is the major atmospheric trace compound responsible for nucleation of aerosol particles in the present-day atmosphere (Dunne et al., 2016). Sulphuric acid participates in new particle formation (NPF) in the upper troposphere (Brock et al., 1995; Weber et al., 1999; Weigel et al., 2011), stratosphere (Deshler, 2008), polar regions (Jokinen et al., 2018), urban or anthropogenic influenced environments (Yao et al., 2018) and when a complex mixture of different condensable vapours is present (Lehtipalo et al., 2018). Especially in the initial growth of small atmospheric molecular clusters, sulphuric acid is likely of crucial importance (Kulmala et al., 2013). The newly formed particles need to grow rapidly in order to avoid scavenging by larger, pre-existing aerosols and, thereby, contribute to the global cloud condensation nuclei (CCN) budget (Pierce and Adams, 2007). The dynamics in this cluster size-range of a few nm therefore determines the climatic significance of atmospheric NPF, which is the major source of CCN (Gordon et al., 2017) and can also affect urban air quality (Guo et al., 2014).

The main pathway of cluster and particle growth is condensation of low volatility vapours, like sulphuric acid or oxidized organics (Stolzenburg et al., 2018). Nanoparticle growth rates depend ~~mainly~~ both on the evaporation rates of the condensing vapours and on the molecular collision frequencies. Uncertainty about the expected behaviour at the collision ("kinetic") limit influences the interpretation of experimental data. One focus has been on evaporation rates from small particles and potential growth-rate enhancement from coagulation. ~~On the one hand, the incomplete understanding of the evaporation and cluster processes in growth lead to the question if growth caused by sulphuric acid proceeds at the kinetic limit of condensation, where~~

2

75 ~~evaporation rates are negligible.~~ It ~~was~~ has been shown in earlier laboratory measurements that bases like ammonia can have a stabilizing effect for growth below 2 nm (Lehtipalo et al., 2016). If amines, which are stronger bases than ammonia, are added, nucleation itself can proceed at the kinetic limit, i.e. evaporation rates from the monomer onwards are zero (Jen et al., 2014; Kürten et al., 2014; Olenius et al., 2013). In this case, cluster coagulation also plays an important role in the growth process due to the strong clustering behaviour of sulphuric acid and amines (Kontkanen et al., 2016; Lehtipalo et al., 2016; Li

80 and McMurry, 2018). However, in the presence of ammonia, the evaporation rates and the magnitude of cluster coagulation remain unmeasured, although ammonia is much more important than amines globally due to its longer atmospheric lifetime. ~~On the other hand, condensation at the kinetic limit is extremely sensitive to molecular-particle collision rates,~~ A second focus is on the collisional rate coefficients themselves, which may be enhanced by either charge-dipole interactions (Nadykto and Yu, 2003) or van-der-Waals forces (Chan and Mozurkewich, 2001). In spite of the importance of these coefficients there are

85 only few ~~, but there are only few~~ direct measurements of the charge effect on growth (Lehtipalo et al., 2016; Svensmark et al., 2017). Even if the charge-dipole interactions are stronger, an enhancement due to van-der-Waals forces might be more important at typical atmospheric ionization levels. Several atmospheric studies have demonstrated that sulphuric acid uptake proceeds close at a collision-limited rate (Bzdek et al., 2013; Kuang et al., 2010), but ~~However,~~ they could ~~not~~ neither provide a measurement of a collision enhancement nor considered in detail hydration effects (Verheggen and Mozurkewich, 2002).~~,~~

90 ~~which will~~ Both might be ~~strongest~~ significant in the free molecular regime below 5 nm, where growth measurements are also affected by larger uncertainties (Kangasluoma and Kontkanen, 2017). Here, we address the questions of ~~of sulphuric acid~~ evaporation~~, cluster contribution~~ and collision enhancement in sulphuric acid driven growth with precision measurements (Stolzenburg et al., 2017) at the CERN (European Organization for Nuclear Research) CLOUD experiment (Duplissy et al., 2016).

95 **2 Methods**

2.1 Experimental approach

The CERN CLOUD chamber is a 26.1 m^3 stainless steel aerosol chamber, which can be kept at a constant temperature within 0.1 K precision. It offers the possibility to study new particle formation under different ionization levels. Two high voltage electrode grids inside the chamber can efficiently clear ions and charged particles from the chamber within seconds, ensuring

100 neutral conditions. When there is no electric field in the chamber galactic cosmic rays lead to an ion production rate of ~2-4 ion pairs cm^{-3} s^{-1}. Ion concentrations can also be elevated to upper tropospheric conditions by illumination of the chamber with a pion beam from the CERN proton-synchrotron. The dry air supply for the chamber is provided by boil-off oxygen and boil-off nitrogen mixed at the atmospheric ratio of 79:21. This ensures extremely low contaminant levels, especially from organics and sulphuric acid. This was verified by a PTR3 proton-transfer-reaction time of flight mass spectrometer (Breitenlechner et

105 al., 2017) and a nitrate chemical ionization-atmospheric pressure interface-time of flight mass spectrometer (nitrate CI-APi-ToF) (Jokinen et al., 2012). The absence of any contamination from amines was confirmed by measurements with a water

cluster-CI-APi-ToF (Pfeifer et al., 2019), which did not register dimethylamine mixing ratios above the detection limit of 0.1 pptv.

We performed measurements of particle growth from sulphuric acid and ammonia at either +20 °C or +5°C with the relative humidity kept constant at either 38% or 60%. SO$_2$ (5 ppb), O$_3$ (~120 ppb) and ammonia (varied between 3 and 1000 pptv) were injected into the chamber. The experiments were initiated by homogeneous illumination of the chamber at constant O$_3$ and SO$_2$ levels. The UV light of four Hamamatsu UV lamps guided into the chamber with fibre optics induced the photo-dissociation of O$_3$ and production of OH· radicals. Thereby, SO$_2$ is oxidized, leading to the formation of sulphuric acid (varied between 10^7 and 10^9 cm^{-3}). A typical experiment is shown in Fig. S1 in the Supplement. Sulphuric acid monomer concentrations were measured with the nitrate CI-API-TOF. Calibration of the instrument's response to sulphuric acid (Kürten et al., 2012) was performed before and after the measurement campaign and yielded comparable results. Compared to previous studies, also the measurement of gas-phase NH$_3$ significantly improved due to the deployment of the calibrated water cluster CI-APi-ToF. The protonated water cluster reagent ions selectively ionize ammonia and amines at ambient pressure reaching a detection limit of approximately 0.5 pptv for ammonia.

Particle growth was monitored using a differential mobility analyser-train (DMA-train) (Stolzenburg et al., 2017) for the main size-range of 1.8-8 nm. We also include measurements from a Caltech nano-radial DMA (Brunelli et al., 2009) with a custom-build DEG-counter for sizes between 4-8 nm and a TSI Model 3936 nano-SMPS for sizes larger than 5 nm when investigating the size-dependency of the growth. For the growth of the charged fraction, we use a neutral cluster and air ion spectrometer (NAIS) (Manninen et al., 2009). All four instruments use electrical mobility classification and measured mobility diameters are corrected to mass diameters (Larriba et al., 2011) for the calculation of collision kinetics. Compared to the scanning particle-size-magnifier (see e.g. Lehtipalo et al., 2014), which was used in Lehtipalo et al. (2016), these instruments using direct mobility analysis have less systematic uncertainty on the actual size classification. The size-ranges of both studies are also not directly comparable. We show the measurements in the lower size-interval of the DMA-train (1.8-3.2 nm mobility diameter) together with the earlier results (size range 1.5-2.5 nm mobility diameter) in Fig. S2 in the Supplement.

Another difference between the instruments is the treatment of the sample relative humidity. In the DMA-train, the aerosol sheath flow is dried by silica gel achieving a relative humidity measured at the sheath inlet of the DMA below 5% for all experiments in this study. The nano-SMPS uses a water trap to keep the relative humidity of the DMA sheath flow below 20 % during the reported experiments. The Caltech nano-radial DMA, the NAIS and the particle size magnifier used in Lehtipalo et al. (2016) do not deploy any humidity conditioning for the sheath or sample flow, except for the possible decrease in relative humidity as a result of a temperature increase between measurement device and chamber. This effect occurred to some extend for all instruments, even if the sampling lines were insulated. The effect of aerosol dehydration during the measurement is usually described by the hygroscopic growth factor gf, relating measured diameter $d_{p,m}$ to the actual diameter d_p via $d_p = $ gf $\cdot d_{p,m}$.

From the measured aerosol size-distributions we inferred particle growth rates with two complementary methods in order to limit systematic biases in the analysis. In the first method, particle growth rates were measured with the appearance time

4

method, requiring a growing particle population, which can be clearly identified (Dada et al., 2020; Lehtipalo et al., 2014; Stolzenburg et al., 2018). Fig. S1d in the Supplement demonstrates how the signal in each size channel is fitted by an empirical sigmoidal shape curve estimating the time where 50 % of the maximum signal intensity is reached. These appearance times are fitted with a linear function over the size intervals 1.8-3.2 nm and 3.2-8 nm, with the slope yielding an average growth rate

145 over the interval, shown in Fig. S1b. In the second method, we applied the size- and time-resolving growth rate analysis method INSIDE (Pichelstorfer et al., 2018) to cross-check our results. The INSIDE method uses the measured particle size distribution at a time t_1 and simulates the expected aerosol dynamics (coagulation, wall losses and dilution) until time t_2. By comparing to the measured data at t_2 and evaluating the general dynamics equation, it infers the condensational growth rate at specified diameters for this time step. The time- and size-resolved growth rates for each experiment were time-averaged for all sizes to

150 yield a statistically more robust result. Compared to the appearance time method, INSIDE requires accurate absolute number size-distributions, while the appearance time method only depends on the relative signal increase. However, INSIDE can confirm the absence of systematic biases like changing precursor vapour concentrations or coagulation and wall loss effects. A combined assessment with both methods should therefore yield a solid estimate of the observed growth rates.

2.2 Growth model description

155 If the evaporation rates of the growing particles are effectively zero due to an extremely low vapour pressure of the condensing vapour, particle growth rates are limited by the collision frequencies of vapour molecules with the growing particles. Our description of particle growth follows the approach of Nieminen et al. (2010), which, in comparison to the equations of mass transfer that can be found in e.g. Seinfeld and Pandis (2016), include the non-negligible effect of vapour molecular size by using a collision frequency between vapour and particle in analogy to coagulation theory (Lehtinen and Kulmala, 2003):

160 $$GR = \frac{\mathrm{d}d_p}{\mathrm{d}t} = \frac{\frac{\mathrm{d}V_p}{\mathrm{d}t}}{\frac{\mathrm{d}V_p}{\mathrm{d}d_p}} = \frac{k_{coll}(d_v,d_p) \cdot V_v \cdot C_v}{\frac{\mathrm{d}}{\mathrm{d}d_p}[\frac{\pi}{6}d_p^3]} = \frac{k_{coll}(d_v,d_p) \cdot V_v \cdot C_v}{\pi/2 \cdot d_p^2}, \tag{1}$$

where d_p is the growing particle mass diameter, V_p and V_v are the volume of particle and vapour molecule, C_v is the vapor monomer concentration and $k_{coll}(d_v, d_p)$ is the kinetic collision frequency between particle and vapour. Following Fuchs and Sutugin (1971), the collision frequency for the transition regime is defined by:

$$k_{coll}(d_v, d_p) = 2\pi \cdot (d_v + d_p) \cdot (D_v + D_p) \cdot \frac{1+Kn}{1+(0.377+\frac{4}{3\alpha})Kn+\frac{4}{3\alpha}Kn^2}, \tag{2}$$

165 where, according to Lehtinen and Kulmala (2003), Knudsen number Kn and mean free path λ need to be specified as $Kn = 2\lambda \cdot (d_v + d_p)^{-1}$ and $\lambda = 3(D_v + D_p) \cdot (\bar{c}_v^2 + \bar{c}_p^2)^{-1/2}$, which depend on the diameters $d_{v/p}$ the masses $m_{v/p}$ (within the calculation of the mean thermal velocities $\bar{c}_{v/p}$) and the diffusion coefficients $D_{v/p}$ of the colliding vapour molecules or particles, respectively. Assuming the accommodation coefficient α is unity and relating the volume V_v of the condensing monomer to its molecular mass and (bulk) density $V_V = m_v/\rho_v$, Eq. (1) and (2) determine the hard-sphere kinetic limit for

170 particle growth.

We then additionally consider a collision enhancement of neutral vapour monomers and particles due to attractive van-der-Waals forces, where the collision frequency can be described according to Sceats (1989):

$$k_{coll}(d_v, d_p) = k_K \cdot \left(\sqrt{1 + \left(\frac{k_K}{2k_D}\right)^2} - \left(\frac{k_K}{2k_D}\right) \right), \tag{3}$$

with and the enhanced collision frequency for the continuum regime:

$$k_D = 2\pi \cdot (d_v + d_p) \cdot (D_v + D_p) \cdot E(0) \tag{4}$$

and the enhanced collision frequency for the kinetic regime:

$$k_K = \frac{\pi}{4} \cdot (d_v + d_p)^2 \cdot \left(\frac{8kT}{\pi}\right)^{1/2} \cdot \left(\frac{1}{m_v} + \frac{1}{m_p}\right)^{1/2} \cdot E(\infty) \tag{5}$$

Eq. (3) is designed such that it reaches the correct limits of the free molecular and diffusion regime comparable to the approach of Fuchs and Sutugin (1971), i.e. Eq. (2). However, it includes collision enhancement factors $E(\infty)$ and $E(0)$. These factors can be linked to the attractive potential of van-der-Waals forces. For the continuum regime, this is done by solving the integral:

$$E(0) = \left[\int_{(r_v + r_p)}^{\infty} \left(\frac{r_v + r_p}{x^2}\right) \exp\left(\frac{\phi(x)}{kT}\right) dx \right]^{-1} \tag{6}$$

where x is the relative distance between the centres of the two colliding entities and $\phi(x)$ is the van-der-Waals potential (Hamaker, 1937), which is expressed in terms of the vapour and particle radii $r_{v/p}$:

$$\frac{\phi(x)}{kT} = -\frac{1}{6} \frac{A}{kT} \left(\frac{2 r_v r_p}{x^2 - (r_v + r_p)^2} + \frac{2 r_v r_p}{x^2 - (r_v - r_p)^2} + \ln\left(\frac{x^2 - (r_v + r_p)^2}{x^2 - (r_v - r_p)^2}\right) \right) \tag{7}$$

Chan and Mozurkewich (2001) provide a fit to the numerical solution of the numerically evaluated integral from Sceats (1989):

$$E(0) = 1 + a_1 \cdot \ln(1 + A') + a_2 \cdot \ln^3(1 + A'), \tag{8}$$

where a_n are the fit parameters and A' is the reduced Hamaker constant, which relates to the Hamaker constant A by $A' = 4A \cdot k^{-1} T^{-1} \cdot d_v d_p \cdot (d_v + d_p)^{-2}$ (Chan and Mozurkewich, 2001; Hamaker, 1937). However, the measurements of this study are conducted completely in the free molecular regime, and hence the derivation of the continuum case will not significantly affect our results. For the free molecular regime enhancement factor $E(\infty)$, an overview of its relation to the Hamaker constant is given in Ouyang et al. (2012). Chan and Mozurkewich (2001) also here used a fit to the solution from Sceats (1989) with the fit parameters b_n:

$$E(\infty) = 1 + \frac{\sqrt{A'/3}}{1 + b_0\sqrt{A'}} + b_1 \cdot \ln(1 + A') + b_2 \cdot \ln^3(1 + A'), \tag{9}$$

In this study, we compare the results of Sceats (1989), who used Brownian coagulation to describe the collisions, to the simple ballistics approach of Fuchs and Sutugin (1965). There, the minimum distance x_{min} along the trajectory of two colliding particles with impact parameter b is calculated from conservation of angular momentum und energy:

$$b = x_{min} \sqrt{1 + \left(\frac{2|\phi(x_{min})|}{\mu v^2}\right)} \tag{10}$$

6

where ϕ is the interaction potential, μ the reduced mass of the colliding entities and v their relative speed. The critical impact parameter b_{crit} is obtained as the minimum value of b for which the minimum distance still takes a real value larger than

200 $(r_v + r_p)$. The enhancement factor is than related to the critical impact parameter b_{crit}:

$$E(\infty) = \frac{4\,b_{\text{crit}}^2}{(d_v+d_p)^2}\sqrt{\frac{3}{2}} \tag{11}$$

Note, that this approach is oversimplified, as the initial velocity of the colliding entities is assumed to be fixed but should actually follow a (Maxwell-Boltzmann) distribution. Ouyang et al. (2012) however concluded that the difference in the derived Hamaker constant is almost negligible.

205 Using the description of an enhanced collision kernel, the particle growth rates measured with the DMA-train can be fitted with the Hamaker constant as the single free parameter of the fit. As the theoretical growth rates are compared to appearance time growth rates, which are measured as a time difference in signal appearance Δt over a certain size-interval Δd_p (ranging from d_{init} to d_{final}), a comparison with experimental values requires integration of Eq. (1):

$$GR\,(d_{\text{init}}, d_{\text{final}}) = \frac{\Delta d_p}{\Delta t} = (d_{\text{final}} - d_{\text{init}})/\int_{d_{\text{init}}}^{d_{\text{final}}} \frac{\pi/2 \cdot d_p^2}{k_{coll}(d_v,d_p) \cdot V_v \cdot C_v}\, \mathrm{d}d_p, \tag{12}$$

210 Eq. (12) includes several properties of the condensing vapour and the growing particles. Sulphuric acid molecules are usually hydrated at typical ambient relative humidity. While the thermodynamic model E-AIM (Wexler et al., 2002) predicts on average 2 water molecules attached to a sulphuric acid monomer at 298 K and 40-60% relative humidity, quantum chemical studies predict 1-2 water molecules average hydration for these conditions (Henschel et al., 2014; Kurtén et al., 2007; Temelso et al., 2012). Moreover, also the hydration state of the particles in the chamber is not directly measured and might be altered

215 during the sampling process, which requires information on the hygroscopic growth factor (see Section 2.1).

We examine the effect of hydration using three different approaches: In a first naïve approach we assume that no dehydration occurs during measurement and the particle sulphuric acid mass fraction is equal to the vapour mass fraction, i.e. $w = M_{H2SO4}/m_v$, with $m_v = M_{H2SO4} + 2M_{H2O}$ (assuming 2 water molecules attached to the sulphuric acid monomer), where M_{H2SO4} and M_{H2O} are the molecular mass of sulphuric acid and water, respectively. In the second approach, we assume

220 a dry measurement, and in this case the growth of the measured dry particles is described by uptake of sulphuric monomers only, i.e. $m_v = M_{H2SO4}$. However, for the actual vapour and particle size used in the collision kernel $k_{coll}(d_v, d_p)$ the hydrated sizes are used. We again assume an average hydration for the monomer with 2 water molecules as above and an average hygroscopic growth factor of 1.25 for all particle sizes and RH values of our experiments. The latter is an average value of the results of Biskos et al. (2009) for highly acidic sulphuric acid sub-10 nm particles at 40-60 % relative humidity.

225 In the third approach, we take into account that the extent of hydration might vary with size and relative humidity. We use modelled composition data from MABNAG (Yli-Juuti et al., 2013) in order to predict the sulfuric acid mass fraction $w(RH, T)$ (see Fig S4a in the Supplement) and calculate the hygroscopic growth factor:

$$gf = \left(\frac{w(RH_m, T_m) \cdot \rho_{sol}(w(RH_m, T_m), T_m)}{w(RH, T) \cdot \rho_{sol}(w(RH, T), T)}\right)^{1/3},\tag{13}$$

where ρ_{sol} is a parametrization of the density of the sulphuric acid water solution (Myhre et al., 1998) and $w(RH, T)$ and $w(RH_m, T_m)$ are the mass fractions of sulphuric acid in the growing and measured particles, respectively. We follow the considerations of Verheggen and Mozurkewich (2002), in order to separate growth by sulphuric acid addition and water uptake by differentiating the hydrated particle volume $V_p = m_{H2SO4}/w\rho_{sol}$. Both, the numerator (particle sulphuric acid mass m_{H2SO4}) and denominator (sulphuric acid mass fraction and solution density) depend on time. The addition of sulphuric acid is again described in analogy to coagulation theory, resulting in:

$$\frac{\pi}{2}d_p^2 \frac{dd_p}{dt} = \frac{k_{coll}(d_v, d_p) \cdot m_v \cdot C_v}{w \cdot \rho} - \frac{\pi d_p^3}{6}\frac{dln(w\rho)}{dt} = \frac{k_{coll}(d_v, d_p) \cdot m_v \cdot C_v}{w \cdot \rho} - \frac{\pi d_p^3}{6}\frac{dln(w\rho)}{dd_p}\frac{dd_p}{dt}\tag{15}$$

Eq. (14) contains a first term for addition of pure sulphuric acid and a second term for water uptake. It can be solved for the particle growth rate $\frac{dd_p}{dt}$:

$$GR = \frac{2 \cdot k_{coll}(d_v, d_p) \cdot m_v \cdot C_v}{w(RH, T) \cdot \rho(RH, T) \cdot \pi \cdot d_p^2 \cdot \left(1 + \frac{d_p}{3} \cdot \frac{dln(w\rho)}{dd_p}\right)},\tag{15}$$

In this case, we assume $m_v = M_{H2SO4}$, but use the hydrated monomer diameter d_v in the collision kernel. For the particles we now use the hydrated size, i.e. $d_p = gf \cdot d_{p,m}$ with gf and $w(RH, T)$ now taken from the model. We compare the MABNAG predictions in Fig. S4b in the Supplement to SAWNUC (Ehrhart et al., 2016), which takes into account only sulphuric acid and water, while MABNAG also includes ammonia. MABNAG predicts a significantly lower water content at larger sizes (>2.5 nm) even at 3 pptv ammonia. In addition, previous experiments in the CLOUD chamber suggested that even background level ammonia has an influence on the hygroscopic growth factor (Kim et al., 2016), similar to Biskos et al. (2009) also indicating some extend of neutralization for sub-10 nm particles at low ammonia. Due to these presumably better prediction of the particle hydration by MABNAG for sizes larger than 2.5 nm, we choose the results of Fig. S4a in the Supplement even if it might overestimate the hydration at small sizes. We neglected the effect of ammonia addition upon collisions in all three approaches so far, but test the assumption $m_v = M_{H2SO4} + 2M_{H2O} + 1M_{NH3}$ together with different vapour hydrations in our systematic uncertainties estimate in Fig. S5 in the Supplement. All used parameters for vapour and particles for all approaches are summarized in Table S1 in the Supplement.

2.3 Global model description

We implement the results of our growth-rate measurements for sulphuric acid driven growth in a global model (Mann et al., 2010; Mulcahy et al., 2018), which includes sulphuric acid-water binary nucleation. However, the model does not include ternary nucleation schemes (Dunne et al., 2016) and pure biogenic nucleation (Gordon et al., 2016) and will therefore underestimate the impact of nucleation on the global aerosol and CCN budget. Here as a baseline case we use the geometric hard-spheres kinetic growth rate based on bulk-density (Eq. (3)) and compare this to the collision enhanced growth (Eq. (4)-(9)). In the model, growth between the nucleation size and 3 nm is treated with the equation of Kerminen and Kulmala

8

(Kerminen and Kulmala, 2002), which gives the fraction of particles surviving to 3 nm at a given growth and loss rate. Here as a baseline case we use the geometric hard-sphere kinetic growth rate based on bulk-density (Eq. (3)) and compare this to the collision enhanced growth (Eq. (4)-(9)). For larger sizes, aerosol growth in the model is calculated by solving the condensation equations. Therefore no direct growth parametrization can be altered, but as condensational growth scales linearly with the diffusion coefficient of the condensing vapour, we increased sulphuric acid diffusion for condensation in the nucleation mode (2-10 nm) and in the Aitken mode (10-100 nm). The enhancement factors are derived for the median diameters of the modes (7.6 and 57 nm respectively) at cloud base level (1 km). However, this constant factor of increase in diffusion coefficient, and hence flux onto particles, for all particles of the entire mode, might underestimate the impact of the collision enhancement. Rapid growth is increasingly important for the smallest particles, which actually have a higher collision enhancement compared to particles with the size of the mode median diameters.

3~~2~~ Results

3.1 Collision enhancement ~~in sulphuric acid growth~~

Figure 1 shows the particle growth rates for two size-intervals (Fig. 1a, 1.8-3.2 nm mobility diameter and Fig. 1b, 3.2-8.0 nm mobility diameter) versus the sulphuric acid monomer concentration, correlating linearly. No significant dependencies on temperature, ionization levels in the chamber or the concentration of ammonia are evident. While the effect of temperature expected from theory is small and cannot be discerned within the statistical uncertainties of our measurements (Nieminen et al., 2010), the insignificant influence of ammonia and ionization level on the growth rate differs from previous findings (Lehtipalo et al., 2016).

We compare the measured growth rates of this study with the results from Lehtipalo et al. (2016) in Fig. S2 in the Supplement. In contrast to our results, elevated ammonia (~ 1000 pptv) led to increased growth rates in that study. The major difference is the narrower size range for the growth-rate measurements (1.5-2.5 nm mobility diameter) due to a different set of instrumentation. For smaller sizes and at low ammonia, sulphuric acid evaporation likely ~~still~~ plays a role due to an increased Kelvin term. The stabilizing effect of ammonia is certainly relevant at the sizes of the nucleating clusters (Kirkby et al., 2011). For our results, we confirm the absence of significant evaporation rates above 2 nm by an independent experiment presented in Fig. 2. It demonstrates that, in the absence of gas-phase sulphuric acid, the coagulation and dilution corrected loss rates of particles ($k_{tot}^{meas} - k_{dil} - k_{coag}^{avg}$) over all sizes follow the expected size-dependence of wall losses which is inferred from the sulphuric acid monomer decay. Evaporation would cause another term distorting the balance equation (also depending on the relative abundances of the particles during the decay), causing a deviation from the expected wall loss rate.

The insignificant effect of ammonia on growth (Fig. 1) and the same high ratio (>100, Fig. S3a in the Supplement) between sulphuric acid monomer and dimer concentrations for all experiments, point towards a negligible influence of clustering ~~, possibly influencing~~on our measured growth rates (Li and McMurry, 2018). Moreover, in Fig. S3b in the Supplement, we

9

290 show with a model including sulphuric acid/ammonia clustering and evaporation, that no cluster contribution is indeed expected even at elevated ammonia concentrations (Kürten, 2019).

In the absence of evaporation and strong clustering, our growth-rate data provide a direct measurement of the condensational

295 growth at the kinetic limit caused by sulphuric acid monomers only. We find the measured growth rates both with and without addition of ammonia to be significantly above the geometric hard-sphere limit (Eq. (1)-(2)) of kinetic condensation (Nieminen et al., 2010). For this comparison we followed a naïve approach, adjusted the measured dry mobility diameters by -0.3 nm to actual mass diameters (Larriba et al., 2011) and then assuming an average hydration of the monomer by 2 water molecules based on quantum chemical calculations (Henschel et al., 2014) together with a size-dependent most probable water content for the

300 growing particles (see Fig. S4a) based on the SAWNUC code (Ehrhart et al., 2016). The derivation of the growth rates from theory and the used parameters are in detail described in the Supplement and listed in Table S1. and applied the resulting mass fraction to find the bulk density (Myhre et al., 1998). The observed enhancement is similar to Lehtipalo et al. (2016) in the case when evaporation was suppressed by ammonia (see Fig. S2). We also measure a growth-rate enhancement for the larger size range (Fig. 1b), which should be less sensitive to evaporation. The faster growth rates might be due to an enhanced

305 collision frequency, which can be attributed to van-der-Waals forces, either permanent dipole-(induced) dipole interactions between polar sulphuric acid molecules and particles or London dispersion forces (London, 1937). We therefore adjusted the condensation equations of Nieminen et al. (2010) with a kinetic collision frequency k_{coll} accounting for an enhancement due to van-der-Waals forces (Chan and Mozurkewich, 2001) (see Supplement). The magnitude of the enhancement is described by the Hamaker constant A (Hamaker, 1937), which we use as the single free parameter to fit a collision enhanced kinetic limit

310 (see Eq. (S9)) to the measured growth rate data. For the Brownian coagulation model linking the Hamaker constant to the collision kernel, i.e. Eq. (4)-(9) (Sceats, 1989), We we find $A = (4.6 \pm 1.5\,(stat.)\,^{+8.1}_{-4.4}\,(syst.)) \cdot 10^{-20}$ J. If we apply a ballistics approach in the free molecular regime (Fuchs and Sutugin, 1965; Ouyang et al., 2012), we derive a slightly higher value of $A = 8.7 \cdot 10^{-20}$ J, but both yield comparable values to ($\pm 1\sigma$ uncertainty) in good agreement with previous results (Chan and Mozurkewich, 2001; McMurry, 1980). While this result uses a Brownian coagulation model to calculate the

315 collision enhancement (Sceats, 1989), we also applied a ballistics approach for the free molecular regime (Fuchs and Sutugin, 1965; Ouyang et al., 2012), and derive a slightly higher value of 1.3·10 -19 J (see Supplement). For both approaches, the enhancement factor for the free molecular regime (2.2 and 2.6, respectively) is comparable to previous experimental results (Kürten et al., 2014; Lehtipalo et al., 2016) and in agreement with quantum chemical calculations (Halonen et al., 2019). The relatively large systematic uncertainties on the Hamaker constant estimate are connected to the systematic uncertainty of the

320 sulphuric acid measurement and to the assumptions on the water content of condensing clusters and growing particles (see Fig. S4b in the Supplement).

An enhancement due to charge-dipole interactions between the polar sulphuric acid monomers and charged particles is not significant in our total (neutral plus charged particle) growth rate measurements, as shown in Fig. 1, where we observe no difference between growth rates under neutral and galactic cosmic ray ionization levels. From average-dipole-orientation theory (Su and Bowers, 1973), a small enhancement is expected in collision frequency ~~even~~ for charged particles above 2 nm ~~is expected~~ (Nadykto and Yu, 2003), which should affect~~ing~~ the growth rate (Laakso et al., 2003; Lehtipalo et al., 2016). We find an enhancement factor of 1.45 by comparing the total to the ion growth rate as shown in Fig. 3, which is in good agreement with theory. However, the total growth rate is influenced on a minor level by the faster ion growth because at the representative galactic cosmic ray ionization levels ~~(ion production rate: ~2-4 ion pairs cm^{-3} s^{-1})~~ and sulphuric acid concentrations in our experiments, most (more than 75%) of the growing particles are neutral (see Fig. 3). However, effects of ion condensation and charge-dipole enhancement might be stronger at lower sulphuric acid concentrations (Svensmark et al., 2017).

3.2 Size-dependency ~~of sulphuric acid growth~~and hydration effect~~s~~

Condensational growth at the geometric kinetic limit predicts increasing growth rates with decreasing particle sizes due to the non-negligible effect of vapour molecule size on the collision cross-section (Nieminen et al., 2010), which, was not yet shown experimentally. Furthermore, the collision enhancement due to van-der-Waals forces and the collision enhancement due to dipole-charge interactions also depend on the comparative size of the condensing vapour and the growing particle. Fig. 4a illustrates the theoretical predictions of the size-dependency of the collision rate of sulphuric acid monomers with larger particles, including van-der-Waals forces and dipole-charge interactions. The enhancement factor compared to the hard-sphere kinetic limit is shown for both the Brownian coagulation model (Sceats, 1989) and the ballistics approach (Fuchs and Sutugin, 1965) (2.1 ~~2~~ and 2.3 for the free molecular regime, respectively) and is comparable to previous experimental results (Kürten et al., 2014; Lehtipalo et al., 2016) and quantum chemical calculations (Halonen et al., 2019).

Besides the approach for calculating the kinetic enhancement factor, also the description of particle hydration might play a crucial role. Up to now, we used the naïve assumption that vapour and particle hydration are the same and that particles are measured at their hydrated size. However, during sampling the measured particles are potentially dried. To investigate the effect of particle hydration, we use the DMA-train data of Fig. 1 to fit the collision enhancement for two alternative approaches, one where we assume that particles are measured dry and one where we separate the uptake of water and sulphuric acid condensation (Verheggen and Mozurkewich, 2002) by using modelled particle composition data from SAWNUC (Ehrhart et al., 2016) or MABNAG (Yli-Juuti et al., 2013). We compare the predictions for the size-dependency of all approaches with the measured growth rates of all instruments normalized to 10^7 cm^{-3} in Fig 4b. ~~Fig. 4b shows the measured size-dependence of all growth rate measurements normalized to a sulphuric acid concentration of 10^7 cm^{-3}.~~ In addition, we ~~calculated~~ show the growth rates using the time- and size-resolving growth rate analysis method INSIDE (Pichelstorfer et al., 2018), which ~~accounts for the effects of coagulation and wall losses and~~ agrees with the appearance time method demonstrating a minor

11

360 systematic bias in our growth rate determination. ~~Both methods clearly show increasing growth rates towards smaller sizes and agree remarkably well, demonstrating that we are not biased by the approach in growth rate determination. The experimental results have a stronger size-dependence than the predicted in the hard-sphere limit. They follow the theoretical predictions including van der Waals forces up to 10 nm, with the approach of Fuchs and Sutugin (1965) slightly better reproducing the measured size dependency. Charge-dipole interactions are not considered here because the charged fraction of the growing particle population is small (Fig. 3) and charge effects only start to dominate below 2 nm (Fig. 4a).~~ All approaches reproduce the size-dependency on an acceptable level (R^2 larger than 0.87). The separation approach yields higher growth rates at the smallest sizes due to the overestimation of hydration by MABNAG below 2.5 nm. For SAWNUC composition data, which presumably describe the cluster hydration better, the R^2 is however only 0.66 not reproducing the
365 observed size-dependency. This is possibly caused by the assumed too high hydration for larger sizes. The simple dry measurement approach might thus be a good approximation to the predictions of both MABNAG and SAWNUC for the size range of interest (see Fig. S4b in the Supplement). We estimate the systematic uncertainty of the results in Fig. S5 in the Supplement, also including the effects of different vapour hydration, ammonia addition and sulphuric acid measurement uncertainty. All approaches overlap largely within their systematic uncertainties with $A = \left(5.2^{+9.7}_{-3.4}(\text{syst.})\right) \cdot 10^{-20}$J as the best
370 estimate of a combined assessment (assuming the Brownian coagulation model). We also give a first order approximation to our measured growth rates and their size-dependency for the conditions of our experiments:

$$GR(\text{nm h}^{-1}) = \left[2.68 \cdot d_p(\text{nm})^{-1.27} + 0.81\right] \cdot \left[H_2SO_4(\text{cm}^{-3}) \cdot 10^{-7}\right] \tag{16}$$

3.3 Global implications

~~Due to~~The observed ~~this~~ steep increase of the growth rates with decreasing size shows that~~,~~ the collision enhancement due to
375 van-der-Waals forces is especially important for the smallest particles. As these are the most vulnerable for losses to pre-existing aerosols, their survival probability in the atmosphere is directly affected, altering the CCN budget (Pierce and Adams, 2007) or promoting new particle formation in urban environments (Kulmala et al., 2017). In order to test the effects of collision enhancement in sulphuric acid growth on a global scale, we use the atmosphere-only configuration of the United Kingdom Earth System Model (UKESM1) (Mulcahy et al., 2018; Walters et al., 2019) which includes the GLOMAP aerosol
380 microphysics module describing nucleation and growth (Mann et al., 2010). Figure 5 illustrates the global model results comparing the baseline case (no collision enhancement) with a collision enhancement simulation (with enhancement factors of 2.2, 1.8 and 1.3 for cluster, nucleation and Aitken mode) for the present-day atmosphere. The absolute particle number concentrations averaged over all longitudes are shown in Figure 5a, indicating changes of more than 50%, especially at high altitudes (>10 km; Figure 5b), where most aerosol particles originate from pure sulphuric-acid driven NPF. The importance of
385 the nucleation process, and therefore the growth-rate enhancement, is lower at lower altitudes and in the northern hemisphere, mainly due to the higher condensation sink and the restriction of the model to only sulphuric acid-water binary nucleation. However, the significant enhancement of sulphuric acid driven nanoparticle growth in the upper troposphere may be important

in quantifying sources of stratospheric aerosols and cirrus cloud condensation nuclei (Brock et al., 1995; Deshler, 2008) and needs to be accounted for in future model development.

390 **4 Discussion**

Understanding nanoparticle growth driven by sulphuric acid is extremely important for modelling the present-day atmosphere. Our measured growth rates cover a wide range of representative atmospheric conditions below 20 °C and reveal that sulphuric acid growth proceeds faster than the geometric hard-sphere kinetic limit. Such faster growth rates in the cluster size range could be in part responsible for the occurrence of NPF in polluted environments (Kulmala et al., 2017). Our results suggest
395 that for sizes larger than 2 nm this collision enhancement due to van-der-Waals forces can be more important than dipole-charge interactions or base-stabilization by ammonia. However, a better knowledge of the ~~uptake of water~~chemical composition of the condensing vapour and growing sub-10 nm particles could further improve our understanding of ~~molecular particle~~molecular -collision rates.

400 For smaller sizes, evaporation of sulphuric acid and charge effects need to be considered ~~(Lehtipalo et al., 2016)~~, but the size-range covered by our measurements is sufficient for the used global model, which nucleates particles at 1.7 nm. We find significantly increased upper tropospheric aerosol concentrations, but the global impact of van-der-Waals forces in nanoparticle growth might be even higher due to the model limitations to binary sulphuric-acid water nucleation.

405 Our results should therefore be considered in future model development, especially when discussing the importance of changing sulphuric acid levels due to reduced anthropogenic emissions of SO_2. Moreover, our parametrization of pure sulphuric acid growth rates will help to identify the contribution to growth of other co-condensing vapours in ambient and laboratory experiments, as they set a new baseline for kinetic condensation of sulphuric acid. Several simplifications have often been applied to kinetic particle growth, including hard-spheres collision based on bulk density and neglect of vapour size
410 to the collision cross section; our results provide clear experimental verification that these simplifications are no longer fit for increasingly accurate measurements at these tiny yet critical sizes.

13

Data availability: All presented datasets are available from the corresponding author upon reasonable request.

Competing interests: The authors declare no competing financial interests.

References

Biskos, G., Buseck, P. R. and Martin, S. T.: Hygroscopic growth of nucleation-mode acidic sulfate particles, J. Aerosol Sci., 40(4), 338–347, doi:https://doi.org/10.1016/j.jaerosci.2008.12.003, 2009.

Breitenlechner, M., Fischer, L., Hainer, M., Heinritzi, M., Curtius, J. and Hansel, A.: PTR3: An Instrument for Studying the Lifecycle of Reactive Organic Carbon in the Atmosphere, Anal. Chem., 89(11), 5824–5831, doi:10.1021/acs.analchem.6b05110, 2017.

Brock, C. A., Hamill, P., Wilson, J. C., Jonsson, H. H. and Chan, K. R.: Particle Formation in the Upper Tropical Troposphere: A Source of Nuclei for the Stratospheric Aerosol, Science (80-.)., 270(5242), 1650–1653, doi:10.1126/science.270.5242.1650, 1995.

Brunelli, N. A., Flagan, R. C. and Giapis, K. P.: Radial Differential Mobility Analyzer for One Nanometer Particle Classification, Aerosol Sci. Tech., 43(1), 53–59, doi:10.1080/02786820802464302, 2009.

Bzdek, B. R., Horan, A. J., Pennington, M. R., DePalma, J. W., Zhao, J., Jen, C. N., Hanson, D. R., Smith, J. N., McMurry, P. H. and Johnston, M. V: Quantitative and time-resolved nanoparticle composition measurements during new particle formation, Faraday Discuss., 165(0), 25–43, doi:10.1039/C3FD00039G, 2013.

Chan, T. W. and Mozurkewich, M.: Measurement of the coagulation rate constant for sulfuric acid particles as a function of particle size using tandem differential mobility analysis, J. Aerosol Sci., 32(3), 321–339, doi:http://dx.doi.org/10.1016/S0021-8502(00)00081-1, 2001.

Dada, L., Lehtipalo, K., Kontkanen, J., Nieminen, T., Baalbaki, R., Ahonen, L., Duplissy, J., Yan, C., Chu, B., Petäjä, T., Lehtinen, K., Kerminen, V.-M., Kulmala, M. and Kangasluoma, J.: Formation and growth of sub-3-nm aerosol particles in experimental chambers, Nat. Protoc., doi:10.1038/s41596-019-0274-z, 2020.

Deshler, T.: A review of global stratospheric aerosol: Measurements, importance, life cycle, and local stratospheric aerosol, Atmos. Res., 90(2), 223–232, doi:https://doi.org/10.1016/j.atmosres.2008.03.016, 2008.

Dunne, E. M., Gordon, H., Kürten, A., Almeida, J., Duplissy, J., Williamson, C., Ortega, I. K., Pringle, K. J., Adamov, A., Baltensperger, U., Barmet, P., Benduhn, F., Bianchi, F., Breitenlechner, M., Clarke, A., Curtius, J., Dommen, J., Donahue, N. M., Ehrhart, S., Flagan, R. C., Franchin, A., Guida, R., Hakala, J., Hansel, A., Heinritzi, M., Jokinen, T., Kangasluoma, J., Kirkby, J., Kulmala, M., Kupc, A., Lawler, M. J., Lehtipalo, K., Makhmutov, V., Mann, G., Mathot, S., Merikanto, J., Miettinen, P., Nenes, A., Onnela, A., Rap, A., Reddington, C. L. S., Riccobono, F., Richards, N. A. D., Rissanen, M. P., Rondo, L., Sarnela, N., Schobesberger, S., Sengupta, K., Simon, M., Sipilä, M., Smith, J. N., Stozhkov, Y., Tomé, A., Tröstl, J., Wagner, P. E., Wimmer, D., Winkler, P. M., Worsnop, D. R. and Carslaw, K. S.: Global atmospheric particle formation from CERN CLOUD measurements, Science, 354(6316), 1119–1124, doi:10.1126/science.aaf2649, 2016.

Duplissy, J., Merikanto, J., Franchin, A., Tsagkogeorgas, G., Kangasluoma, J., Wimmer, D., Vuollekoski, H., Schobesberger, S., Lehtipalo, K., Flagan, R. C., Brus, D., Donahue, N. M., Vehkamäki, H., Almeida, J., Amorim, A., Barmet, P., Bianchi, F., Breitenlechner, M., Dunne, E. M., Guida, R., Henschel, H., Junninen, H., Kirkby, J., Kürten, A., Kupc, A., Määttänen, A., Makhmutov, V., Mathot, S., Nieminen, T., Onnela, A., Praplan, A. P., Riccobono, F., Rondo, L., Steiner, G., Tome, A., Walther, H., Baltensperger, U., Carslaw, K. S., Dommen, J., Hansel, A., Petäjä, T., Sipilä, M., Stratmann, F., Vrtala, A., Wagner, P. E., Worsnop, D. R., Curtius, J. and Kulmala, M.: Effect of ions on sulfuric acid-water binary particle formation: 2. Experimental data and comparison with QC-normalized classical nucleation theory, J. Geophys. Res.-Atmos., 121(4), 1752–

1775, doi:10.1002/2015JD023539, 2016.

Ehrhart, S., Ickes, L., Almeida, J., Amorim, A., Barmet, P., Bianchi, F., Dommen, J., Dunne, E. M., Duplissy, J., Franchin, A., Kangasluoma, J., Kirkby, J., Kürten, A., Kupc, A., Lehtipalo, K., Nieminen, T., Riccobono, F., Rondo, L., Schobesberger, S.,

475 Steiner, G., Tomé, A., Wimmer, D., Baltensperger, U., Wagner, P. E. and Curtius, J.: Comparison of the SAWNUC model with CLOUD measurements of sulphuric acid-water nucleation, J. Geophys. Res.-Atmos., 121(20), 12,401-12,414, doi:10.1002/2015JD023723, 2016.

Fuchs, N. A. and Sutugin, A. G.: Coagulation rate of highly dispersed aerosols, J. Colloid Sci., 20(6), 492–500, doi:https://doi.org/10.1016/0095-8522(65)90031-0, 1965.

480 Fuchs, N. A. and Sutugin, A. G.: High dispersed aerosols, in Topics in Current Aerosol Research (Part 2), edited by G. M. Hidy and J. R. Brock, pp. 1–200, Pergamon, New York., 1971.

Gordon, H., Sengupta, K., Rap, A., Duplissy, J., Frege, C., Williamson, C., Heinritzi, M., Simon, M., Yan, C., Almeida, J., Tröstl, J., Nieminen, T., Ortega, I. K., Wagner, R., Dunne, E. M., Adamov, A., Amorim, A., Bernhammer, A.-K., Bianchi, F., Breitenlechner, M., Brilke, S., Chen, X., Craven, J. S., Dias, A., Ehrhart, S., Fischer, L., Flagan, R. C., Franchin, A., Fuchs,

485 C., Guida, R., Hakala, J., Hoyle, C. R., Jokinen, T., Junninen, H., Kangasluoma, J., Kim, J., Kirkby, J., Krapf, M., Kürten, A., Laaksonen, A., Lehtipalo, K., Makhmutov, V., Mathot, S., Molteni, U., Monks, S. A., Onnela, A., Peräkylä, O., Piel, F., Petäjä, T., Praplan, A. P., Pringle, K. J., Richards, N. A. D., Rissanen, M. P., Rondo, L., Sarnela, N., Schobesberger, S., Scott, C. E., Seinfeld, J. H., Sharma, S., Sipilä, M., Steiner, G., Stozhkov, Y., Stratmann, F., Tomé, A., Virtanen, A., Vogel, A. L., Wagner, A. C., Wagner, P. E., Weingartner, E., Wimmer, D., Winkler, P. M., Ye, P., Zhang, X., Hansel, A., Dommen, J., Donahue, N.

490 M., Worsnop, D. R., Baltensperger, U., Kulmala, M., Curtius, J. and Carslaw, K. S.: Reduced anthropogenic aerosol radiative forcing caused by biogenic new particle formation, P. Nat. Acad. Sci. USA, 113(43), 12053–12058, doi:10.1073/pnas.1602360113, 2016.

Gordon, H., Kirkby, J., Baltensperger, U., Bianchi, F., Breitenlechner, M., Curtius, J., Dias, A., Dommen, J., Donahue, N. M., Dunne, E. M., Duplissy, J., Ehrhart, S., Flagan, R. C., Frege, C., Fuchs, C., Hansel, A., Hoyle, C. R., Kulmala, M., Kürten, A.,

495 Lehtipalo, K., Makhmutov, V., Molteni, U., Rissanen, M. P., Stozhkov, Y., Tröstl, J., Tsagkogeorgas, G., Wagner, R., Williamson, C., Wimmer, D., Winkler, P. M., Yan, C. and Carslaw, K. S.: Causes and importance of new particle formation in the present-day and preindustrial atmospheres, J. Geophys. Res.-Atmos., 122, doi:10.1002/2017JD026844, 2017.

Guo, S., Hu, M., Zamora, M. L., Peng, J., Shang, D., Zheng, J., Du, Z., Wu, Z., Shao, M., Zeng, L., Molina, M. J. and Zhang, R.: Elucidating severe urban haze formation in China, P. Nat. Acad. Sci. USA, 111(49), 17373 LP – 17378,

500 doi:10.1073/pnas.1419604111, 2014.

Halonen, R., Zapadinsky, E., Kurtén, T., Vehkamäki, H. and Reischl, B.: Rate enhancement in collisions of sulfuric acid molecules due to long-range intermolecular forces, Atmos. Chem. Phys., 19, 13355–13366, doi:10.5194/acp-19-13355-2019,

2019.

Hamaker, H. C.: The London—van der Waals attraction between spherical particles, Physica, 4(10), 1058–1072,
doi:https://doi.org/10.1016/S0031-8914(37)80203-7, 1937.

Henschel, H., Navarro, J. C. A., Yli-Juuti, T., Kupiainen-Määttä, O., Olenius, T., Ortega, I. K., Clegg, S. L., Kurtén, T.,
Riipinen, I. and Vehkamäki, H.: Hydration of Atmospherically Relevant Molecular Clusters: Computational Chemistry and
Classical Thermodynamics, J. Phys. Chem. A, 118(14), 2599–2611, doi:10.1021/jp500712y, 2014.

Jen, C. N., McMurry, P. H. and Hanson, D. R.: Stabilization of sulfuric acid dimers by ammonia, methylamine, dimethylamine,
and trimethylamine, J. Geophys. Res.-Atmos., 119(12), 7502–7514, doi:10.1002/2014JD021592, 2014.

Jokinen, T., Sipilä, M., Junninen, H., Ehn, M., Lönn, G., Hakala, J., Petäjä, T., Mauldin III, R. L., Kulmala, M. and Worsnop,
D. R.: Atmospheric sulphuric acid and neutral cluster measurements using CI-APi-TOF, Atmos. Chem. Phys., 12(9), 4117–
4125, doi:10.5194/acp-12-4117-2012, 2012.

Jokinen, T., Sipilä, M., Kontkanen, J., Vakkari, V., Tisler, P., Duplissy, E. and Junninen, H.: Ion-induced sulfuric acid –
ammonia nucleation drives particle formation in coastal Antarctica, Sci. Adv., 1–7, 2018.

Kangasluoma, J. and Kontkanen, J.: On the sources of uncertainty in the sub-3nm particle concentration measurement, J.
Aerosol Sci., 112(Supplement C), 34–51, doi:https://doi.org/10.1016/j.jaerosci.2017.07.002, 2017.

Kerminen, V.-M. and Kulmala, M.: Analytical formulae connecting the "real" and the "apparent" nucleation rate and the nuclei
number concentration for atmospheric nucleation events, J. Aerosol Sci., 33(4), 609–622, doi:10.1016/S0021-8502(01)00194-
X, 2002.

Kim, J., Ahlm, L., Yli-Juuti, T., Lawler, M., Keskinen, H., Tröstl, J., Schobesberger, S., Duplissy, J., Amorim, A., Bianchi,
F., Donahue, N. M., Flagan, R. C., Hakala, J., Heinritzi, M., Jokinen, T., Kürten, A., Laaksonen, A., Lehtipalo, K., Miettinen,
P., Petäjä, T., Rissanen, M. P., Rondo, L., Sengupta, K., Simon, M., Tomé, A., Williamson, C., Wimmer, D., Winkler, P. M.,
Ehrhart, S., Ye, P., Kirkby, J., Curtius, J., Baltensperger, U., Kulmala, M., Lehtinen, K. E. J., Smith, J. N., Riipinen, I. and
Virtanen, A.: Hygroscopicity of nanoparticles produced from homogeneous nucleation in the CLOUD experiments, Atmos.
Chem. Phys., 16(1), 293–304, doi:10.5194/acp-16-293-2016, 2016.

Kirkby, J., Curtius, J., Almeida, J., Dunne, E., Duplissy, J., Ehrhart, S., Franchin, A., Gagné, S., Ickes, L., Kürten, A., Kupc,
A., Metzger, A., Riccobono, F., Rondo, L., Schobesberger, S., Tsagkogeorgas, G., Wimmer, D., Amorim, A., Bianchi, F.,
Breitenlechner, M., David, A., Dommen, J., Downard, A., Ehn, M., Flagan, R. C., Haider, S., Hansel, A., Hauser, D., Jud, W.,
Junninen, H., Kreissl, F., Kvashin, A., Laaksonen, A., Lehtipalo, K., Lima, J., Lovejoy, E. R., Makhmutov, V., Mathot, S.,
Mikkilä, J., Minginette, P., Mogo, S., Nieminen, T., Onnela, A., Pereira, P., Petäjä, T., Schnitzhofer, R., Seinfeld, J. H., Sipilä,
M., Stozhkov, Y., Stratmann, F., Tomé, A., Vanhanen, J., Viisanen, Y., Vrtala, A., Wagner, P. E., Walther, H., Weingartner,

E., Wex, H., Winkler, P. M., Carslaw, K. S., Worsnop, D. R., Baltensperger, U. and Kulmala, M.: Role of sulphuric acid, ammonia and galactic cosmic rays in atmospheric aerosol nucleation, Nature, 476, 429–433, doi:10.1038/nature10343, 2011.

535 Kontkanen, J., Olenius, T., Lehtipalo, K., Vehkamäki, H., Kulmala, M. and Lehtinen, K. E. J.: Growth of atmospheric clusters involving cluster-cluster collisions: comparison of different growth rate methods, Atmos. Chem. Phys., 16(9), 5545–5560, doi:10.5194/acp-16-5545-2016, 2016.

Kuang, C., Riipinen, I., Sihto, S.-L., Kulmala, M., McCormick, A. V and McMurry, P. H.: An improved criterion for new particle formation in diverse atmospheric environments, Atmos. Chem. Phys., 10(17), 8469–8480, doi:10.5194/acp-10-8469-540 2010, 2010.

Kulmala, M., Kontkanen, J., Junninen, H., Lehtipalo, K., Manninen, H. E., Nieminen, T., Petäjä, T., Sipilä M., M., Schobesberger, S., Rantala, P., Franchin, A., Jokinen, T., Järvinen, E., Äijälä, M., Kangasluoma, J., Hakala, J., Aalto, P. P., Paasonen, P., Mikkilä, J., Vanhanen, J., Aalto, J., Hakola, H., Makkonen, U., Ruuskanen, T., Mauldin, R. L., Duplissy, J., Vehkamäki, H., Bäck, J., Kortelainen, A., Riipinen, I., Kurtén, T., Johnston, M. V, Smith, J. N., Ehn, M., Mentel, T. F., 545 Lehtinen, K. E. J., Laaksonen, A., Kerminen, V.-M. and Worsnop, D. R.: Direct Observations of Atmospheric Aerosol Nucleation, Science, 339(6122), 943–946, doi:10.1126/science.1227385, 2013.

Kulmala, M., Kerminen, V.-M., Petäjä, T., Ding, A. J. and Wang, L.: Atmospheric gas-to-particle conversion: why NPF events are observed in megacities?, Faraday Discuss., 200(0), 271–288 [online] Available from: http://dx.doi.org/10.1039/C6FD00257A, 2017.

550 Kürten, A.: New particle formation from sulfuric acid and ammonia: nucleation and growth model based on thermodynamics derived from CLOUD measurements for a wide range of conditions, Atmos. Chem. Phys., 19(7), 5033–5050, doi:10.5194/acp-19-5033-2019, 2019.

Kürten, A., Rondo, L., Ehrhart, S. and Curtius, J.: Calibration of a Chemical Ionization Mass Spectrometer for the Measurement of Gaseous Sulfuric Acid, J. Phys. Chem. A, 116(24), 6375–6386, doi:10.1021/jp212123n, 2012.

555 Kürten, A., Jokinen, T., Simon, M., Sipilä, M., Sarnela, N., Junninen, H., Adamov, A., Almeida, J., Amorim, A., Bianchi, F., Breitenlechner, M., Dommen, J., Donahue, N. M., Duplissy, J., Ehrhart, S., Flagan, R. C., Franchin, A., Hakala, J., Hansel, A., Heinritzi, M., Hutterli, M., Kangasluoma, J., Kirkby, J., Laaksonen, A., Lehtipalo, K., Leiminger, M., Makhmutov, V., Mathot, S., Onnela, A., Petäjä, T., Praplan, A. P., Riccobono, F., Rissanen, M. P., Rondo, L., Schobesberger, S., Seinfeld, J. H., Steiner, G., Tomé, A., Tröstl, J., Winkler, P. M., Williamson, C., Wimmer, D., Ye, P., Baltensperger, U., Carslaw, K. S., Kulmala, M., 560 Worsnop, D. R. and Curtius, J.: Neutral molecular cluster formation of sulfuric acid–dimethylamine observed in real time under atmospheric conditions, P. Nat. Acad. Sci. USA, 111(42), 15019–15024, doi:10.1073/pnas.1404853111, 2014.

Kurtén, T., Noppel, M., Vehkamäki, H., Salonen, M. and Kulmala, M.: Quantum chemical studies of hydrate formation of

18

H2SO4 and HSO4-, Boreal Environ. Res., 12(3), 431–453, 2007.

Laakso, L., Kulmala, M. and Lehtinen, K. E. J.: Effect of condensation rate enhancement factor on 3-nm (diameter) particle

565   formation in binary ion-induced and homogeneous nucleation, J. Geophys. Res.-Atmos., 108(D18), doi:10.1029/2003JD003432, 2003.

Larriba, C., Jr., C. J. H., Attoui, M., Borrajo, R., Garcia, J. F. and de la Mora, J. F.: The Mobility–Volume Relationship below 3.0 nm Examined by Tandem Mobility–Mass Measurement, Aerosol Sci. Tech., 45(4), 453–467, doi:10.1080/02786826.2010.546820, 2011.

570   Lehtinen, K. E. J. and Kulmala, M.: A model for particle formation and growth in the atmosphere with molecular resolution in size, Atmos. Chem. Phys., 3(1), 251–257, doi:10.5194/acp-3-251-2003, 2003.

Lehtipalo, K., Leppä, J., Kontkanen, J., Kangasluoma, J., Franchin, A., Wimmer, D., Schobesberger, S., Junninen, H., Petäjä, T., Sipilä, M., Mikkilä, J., Vanhanen, J., Worsnop, D. R. and Kulmala, M.: Methods for determining particle size distribution and growth rates between 1 and 3 nm using the Particle Size Magnifier, Boreal Environ. Res., 19(suppl. B), 215–236, 2014.

575   Lehtipalo, K., Rondo, L., Kontkanen, J., Schobesberger, S., Jokinen, T., Sarnela, N., Kürten, A., Ehrhart, S., Franchin, A., Nieminen, T., Riccobono, F., Sipilä, M., Yli-Juuti, T., Duplissy, J., Adamov, A., Ahlm, L., Almeida, J., Amorim, A., Bianchi, F., Breitenlechner, M., Dommen, J., Downard, A. J., Dunne, E. M., Flagan, R. C., Guida, R., Hakala, J., Hansel, A., Jud, W., Kangasluoma, J., Kerminen, V.-M., Keskinen, H., Kim, J., Kirkby, J., Kupc, A., Kupiainen-Määttä, O., Laaksonen, A., Lawler, M. J., Leiminger, M., Mathot, S., Olenius, T., Ortega, I. K., Onnela, A., Petäjä, T., Praplan, A., Rissanen, M. P., Ruuskanen,

580   T., Santos, F. D., Schallhart, S., Schnitzhofer, R., Simon, M., Smith, J. N., Tröstl, J., Tsagkogeorgas, G., Tomé, A., Vaattovaara, P., Vehkamäki, H., Vrtala, A. E., Wagner, P. E., Williamson, C., Wimmer, D., Winkler, P. M., Virtanen, A., Donahue, N. M., Carslaw, K. S., Baltensperger, U., Riipinen, I., Curtius, J., Worsnop, D. R. and Kulmala, M.: The effect of acid–base clustering and ions on the growth of atmospheric nano-particles, Nat. Commun., 7, 11594, doi:10.1038/ncomms11594, 2016.

585   Lehtipalo, K., Yan, C., Dada, L., Bianchi, F., Xiao, M., Wagner, R., Stolzenburg, D., Ahonen, L. R., Amorim, A., Baccarini, A., Bauer, P. S., Baumgartner, B., Bergen, A., Bernhammer, A.-K., Breitenlechner, M., Brilke, S., Buchholz, A., Mazon, S. B., Chen, D., Chen, X., Dias, A., Dommen, J., Draper, D. C., Duplissy, J., Ehn, M., Finkenzeller, H., Fischer, L., Frege, C., Fuchs, C., Garmash, O., Gordon, H., Hakala, J., He, X., Heikkinen, L., Heinritzi, M., Helm, J. C., Hofbauer, V., Hoyle, C. R., Jokinen, T., Kangasluoma, J., Kerminen, V.-M., Kim, C., Kirkby, J., Kontkanen, J., Kürten, A., Lawler, M. J., Mai, H., Mathot,

590   S., Mauldin, R. L., Molteni, U., Nichman, L., Nie, W., Nieminen, T., Ojdanic, A., Onnela, A., Passananti, M., Petäjä, T., Piel, F., Pospisilova, V., Quéléver, L. L. J., Rissanen, M. P., Rose, C., Sarnela, N., Schallhart, S., Schuchmann, S., Sengupta, K., Simon, M., Sipilä, M., Tauber, C., Tomé, A., Tröstl, J., Väisänen, O., Vogel, A. L., Volkamer, R., Wagner, A. C., Wang, M., Weitz, L., Wimmer, D., Ye, P., Ylisirniö, A., Zha, Q., Carslaw, K. S., Curtius, J., Donahue, N. M., Flagan, R. C., Hansel, A.,

Riipinen, I., Virtanen, A., Winkler, P. M., Baltensperger, U., Kulmala, M. and Worsnop, D. R.: Multicomponent new particle formation from sulfuric acid, ammonia, and biogenic vapors, Sci. Adv., 4(12), eaau5363, doi:10.1126/sciadv.aau5363, 2018.

Li, C. and McMurry, P. H.: Errors in nanoparticle growth rates inferred from measurements in chemically reacting aerosol systems, Atmos. Chem. Phys., 18, 8979–8993, doi:10.5194/acp-18-8979-2018, 2018.

London, F.: The general theory of molecular forces, Trans. Faraday Soc., 33(0), 8b – 26, doi:10.1039/TF937330008B, 1937.

Mann, G. W., Carslaw, K. S., Spracklen, D. V., Ridley, D. A., Manktelow, P. T., Chipperfield, M. P., Pickering, S. J. and Johnson, C. E.: Description and evaluation of GLOMAP-mode: A modal global aerosol microphysics model for the UKCA composition-climate model, Geosci. Model Dev., 3(2), 519–551, doi:10.5194/gmd-3-519-2010, 2010.

Manninen, H. E., Petäjä, T., Asmi, E., Riipinen, I., Nieminen, T., Mikkilä, J., Hõrrak, U., Mirme, A., Mirme, S., Laakso, L., Kerminen, V.-M. and Kulmala, M.: Long-term field measurements of charged and neutral clusters using Neutral cluster and Air Ion Spectrometer (NAIS), Boreal Environ. Res, 14, 591–605, 2009.

McMurry, P. H.: Photochemical aerosol formation from SO2: A theoretical analysis of smog chamber data, J. Colloid Interf. Sci., 78(2), 513–527, doi:10.1016/0021-9797(80)90589-5, 1980.

Mulcahy, J. P., Jones, C., Sellar, A., Johnson, B., Boutle, I. A., Jones, A., Andrews, T., Rumbold, S. T., Mollard, J., Bellouin, N., Johnson, C. E. and Williams, K. D.: Improved Aerosol Processes and Effective Radiative Forcing in HadGEM3 and UKESM1, J. Adv. Model Earth Sy., 10, 2786–2805, doi:10.1029/2018MS001464, 2018.

Myhre, C. E. L., Nielsen, C. J. and Saastad, O. W.: Density and Surface Tension of Aqueous H2SO4 at Low Temperature, J. Chem. Eng. Data, 43(4), 617–622, doi:10.1021/je980013g, 1998.

Nadykto, A. B. and Yu, F.: Uptake of neutral polar vapor molecules by charged clusters/particles: Enhancement due to dipole-charge interaction, J. Geophys. Res.-Atmos., 108(D23), doi:10.1029/2003JD003664, 2003.

Nieminen, T., Lehtinen, K. E. J. and Kulmala, M.: Sub-10 nm particle growth by vapor condensation – effects of vapor molecule size and particle thermal speed, Atmos. Chem. Phys., 10(20), 9773–9779, doi:10.5194/acp-10-9773-2010, 2010.

Olenius, T., Ortega, I. K., Kurtén, T., Vehkamäki, H., Olenius, T., Kupiainen-määttä, O., Ortega, I. K., Kurtén, T. and Vehkamäki, H.: Free energy barrier in the growth of sulfuric acid – ammonia and sulfuric acid – dimethylamine clusters, J. Chem. Phys., 139(8), 084312, doi:10.1063/1.4819024, 2013.

Ouyang, H., Gopalakrishnan, R. and Hogan, C. J.: Nanoparticle collisions in the gas phase in the presence of singular contact potentials, J. Chem. Phys., 137(6), 64316, doi:10.1063/1.4742064, 2012.

Pfeifer, J., Simon, M., Heinritzi, M., Piel, F., Weitz, L., Wang, D., Granzin, M., Müller, T., Bräkling, S., Kirkby, J., Curtius,

J. and Kürten, A.: Measurement of ammonia, amines and iodine species using protonated water cluster chemical ionization mass spectrometry, Atmos. Meas. Tech. Discuss., 2019, 1–36, doi:10.5194/amt-2019-215, 2019.

625 Pichelstorfer, L., Stolzenburg, D., Ortega, J., Karl, T., Kokkola, H., Laakso, A., Lehtinen, K. E. J., Smith, J. N., McMurry, P. H. and Winkler, P. M.: Resolving nanoparticle growth mechanisms from size- and time-dependent growth rate analysis, Atmos. Chem. Phys., 18(2), 1307–1323, doi:10.5194/acp-18-1307-2018, 2018.

Pierce, J. R. and Adams, P. J.: Efficiency of cloud condensation nuclei formation from ultrafine particles, Atmos. Chem. Phys., 7(5), 1367–1379, doi:10.5194/acp-7-1367-2007, 2007.

Sceats, M. G.: Brownian coagulation in aerosols-the role of long range forces, J. Colloid Interf. Sci., 129(1), 105–112,
630 doi:https://doi.org/10.1016/0021-9797(89)90419-0, 1989.

Seinfeld, J. and Pandis, S.: Atmospheric Chemistry and Physics: From Air Pollution to Climate Change, 3rd edition, 3rd editio., Wiley., 2016.

Stolzenburg, D., Steiner, G. and Winkler, P. M.: A DMA-train for precision measurement of sub-10 nm aerosol dynamics, Atmos. Meas. Tech., 10(4), 1639–1651, doi:10.5194/amt-10-1639-2017, 2017.

635 Stolzenburg, D., Fischer, L., Vogel, A. L., Heinritzi, M., Schervish, M., Simon, M., Wagner, A. C., Dada, L., Ahonen, L. R., Amorim, A., Baccarini, A., Bauer, P. S., Baumgartner, B., Bergen, A., Bianchi, F., Breitenlechner, M., Brilke, S., Buenrostro Mazon, S., Chen, D., Dias, A., Draper, D. C., Duplissy, J., El Haddad, I., Finkenzeller, H., Frege, C., Fuchs, C., Garmash, O., Gordon, H., He, X., Helm, J., Hofbauer, V., Hoyle, C. R., Kim, C., Kirkby, J., Kontkanen, J., Kürten, A., Lampilahti, J., Lawler, M., Lehtipalo, K., Leiminger, M., Mai, H., Mathot, S., Mentler, B., Molteni, U., Nie, W., Nieminen, T., Nowak, J. B.,
640 Ojdanic, A., Onnela, A., Passananti, M., Petäjä, T., Quéléver, L. L. J., Rissanen, M. P., Sarnela, N., Schallhart, S., Tauber, C., Tomé, A., Wagner, R., Wang, M., Weitz, L., Wimmer, D., Xiao, M., Yan, C., Ye, P., Zha, Q., Baltensperger, U., Curtius, J., Dommen, J., Flagan, R. C., Kulmala, M., Smith, J. N., Worsnop, D. R., Hansel, A., Donahue, N. M. and Winkler, P. M.: Rapid growth of organic aerosol nanoparticles over a wide tropospheric temperature range, P. Nat. Acad. Sci. USA, 115(37), 9122–9127, doi:10.1073/pnas.1807604115, 2018.

645 Su, T. and Bowers, M. T.: Theory of ion-polar molecule collisions. Comparison with experimental charge transfer reactions of rare gas ions to geometric isomers of difluorobenzene and dichloroethylene, J. Chem. Phys., 58(7), 3027–3037, doi:10.1063/1.1679615, 1973.

Svensmark, H., Enghoff, M. B., Shaviv, N. J. and Svensmark, J.: Increased ionization supports growth of aerosols into cloud condensation nuclei, Nat. Commun., 8, 2199, doi:10.1038/s41467-017-02082-2, 2017.

650 Temelso, B., Morrell, T. E., Shields, R. M., Allodi, M. A., Wood, E. K., Kirschner, K. N., Castonguay, T. C., Archer, K. A. and Shields, G. C.: Quantum Mechanical Study of Sulfuric Acid Hydration: Atmospheric Implications, J. Phys. Chem. A,

116(9), 2209–2224, doi:10.1021/jp2119026, 2012.

Verheggen, B. and Mozurkewich, M.: Determination of nucleation and growth rates from observation of a SO2 induced atmospheric nucleation event, J. Geophys. Res.-Atmos., 107(D11), AAC 5-1-AAC 5-12, doi:10.1029/2001JD000683, 2002.

655   Walters, D., Baran, A. J., Boutle, I., Brooks, M., Earnshaw, P., Edwards, J., Furtado, K., Hill, P., Lock, A., Manners, J., Morcrette, C., Mulcahy, J., Sanchez, C., Smith, C., Stratton, R., Tennant, W., Tomassini, L., Van Weverberg, K., Vosper, S., Willett, M., Browse, J., Bushell, A., Carslaw, K., Dalvi, M., Essery, R., Gedney, N., Hardiman, S., Johnson, B., Johnson, C., Jones, A., Jones, C., Mann, G., Milton, S., Rumbold, H., Sellar, A., Ujiie, M., Whitall, M., Williams, K. and Zerroukat, M.: The Met Office Unified Model Global Atmosphere 7.0/7.1 and JULES Global Land 7.0 configurations, Geosci. Model Dev.,

660   12(5), 1909–1963, doi:10.5194/gmd-12-1909-2019, 2019.

Weber, R. J., McMurry, P. H., Mauldin, R. L., Tanner, D. J., Eisele, F. L., Clarke, A. D. and Kapustin, V. N.: New particle formation in the remote troposphere: A comparison of observations at various sites, Geophys. Res. Lett., 26(3), 307–310, doi:10.1029/1998GL900308, 1999.

Weigel, R., Borrmann, S., Kazil, J., Minikin, A., Stohl, A., Wilson, J. C., Reeves, J. M., Kunkel, D., De Reus, M., Frey, W.,

665   Lovejoy, E. R., Volk, C. M., Viciani, S., D'Amato, F., Schiller, C., Peter, T., Schlager, H., Cairo, F., Law, K. S., Shur, G. N., Belyaev, G. V. and Curtius, J.: In situ observations of new particle formation in the tropical upper troposphere: The role of clouds and the nucleation mechanism, Atmos. Chem. Phys., 11(18), 9983–10010, doi:10.5194/acp-11-9983-2011, 2011.

Yao, L., Garmash, O., Bianchi, F., Zheng, J., Yan, C., Kontkanen, J., Junninen, H., Mazon, S. B., Ehn, M., Paasonen, P., Sipilä, M., Wang, M., Wang, X., Xiao, S., Chen, H., Lu, Y., Zhang, B., Wang, D., Fu, Q., Geng, F., Li, L., Wang, H., Qiao, L., Yang,

670   X., Chen, J., Kerminen, V.-M., Petäjä, T., Worsnop, D. R., Kulmala, M. and Wang, L.: Atmospheric new particle formation from sulfuric acid and amines in a Chinese megacity, Science, 361(6399), 278–281, doi:10.1126/science.aao4839, 2018.

Yli-Juuti, T., Barsanti, K., Hildebrandt Ruiz, L., Kieloaho, A.-J., Makkonen, U., Petäjä, T., Ruuskanen, T., Kulmala, M. and Riipinen, I.: Model for acid-base chemistry in nanoparticle growth (MABNAG), Atmos. Chem. Phys., 13(24), 12507–12524, doi:10.5194/acp-13-12507-2013, 2013.
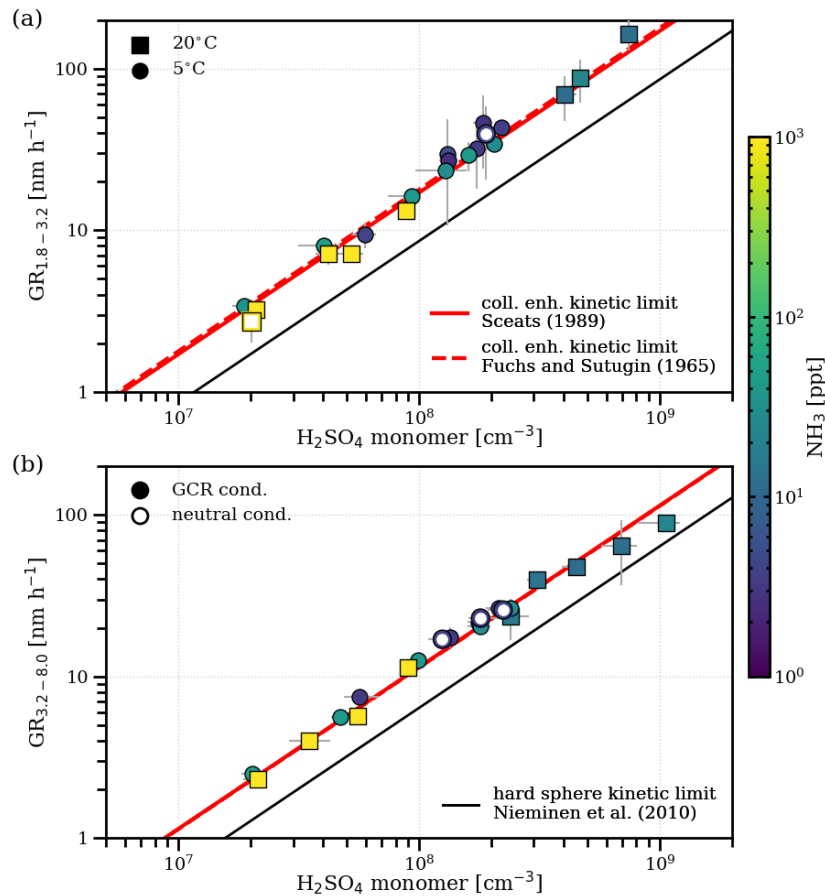
Figure 1: ~~Growth Rate Measurements.~~ Growth rates of nanoparticles in two size-intervals versus measured gas-phase sulphuric acid monomer concentration. (a) shows growth rates for the size-interval between 1.8-3.2 nm (mobility diameter; 1.5-2.9 nm in mass diameter), while (b) shows the growth rates for the size-interval 3.2-8.0 nm (mobility diameter, 2.9-7.7 nm in mass diameter). The colour code represents the measured NH_3 concentration during the growth period. Squares are measurements at 20°C, circles at 5°C. Filled symbols represent runs under ambient galactic cosmic ray ionization levels, and open symbols under neutral conditions. Error bars for the data points represent the statistical uncertainty in the appearance time growth rate measurements and ~~in y-direction. In x-direction, they represent~~ the maximum variation of the sulphuric acid concentration during the growth period ~~in the corresponding interval~~, also explaining the slight deviations from linearity at high sulphuric acid concentrations, where stable conditions are not fully reached. The ~~dashed~~ black line ~~and shaded grey area~~ show the geometric limit of kinetic ~~condensation and the corresponding systematic uncertainty based on the~~ assum~~ed~~ing the same hydration for ~~water content of~~ the condensing cluster and ~~growing~~ the measured particles (Nieminen et al., 2010)~~., while t~~The red solid line shows the fit of Eq. (~~1~~12) to the data with the Hamaker constant as free parameter assuming a Brownian coagulation model for the enhanced collision kernel (Sceats, 1989), while the red dashed line uses a ballistics approach (Fuchs and Sutugin, 1965).

23
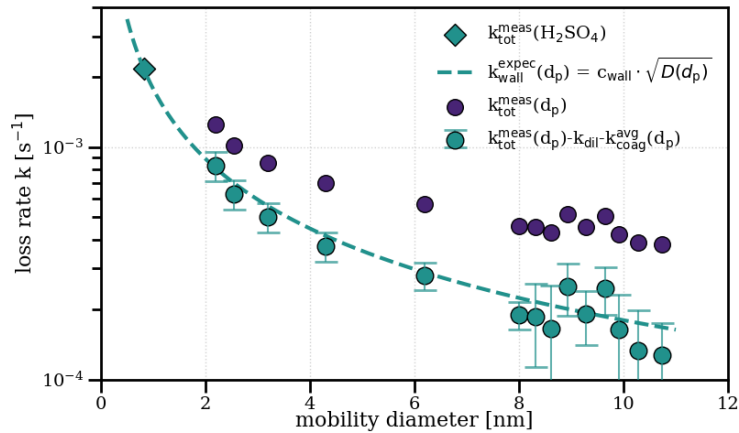
Figure 2: Measurement of zero sulphuric acid evaporation rates. Total loss rates of sulphuric acid and ammonia particles with mobility diameter shown on the x-axis measured during a decay experiment (5°C, 60% relative humidity, 1000 pptv NH$_3$), by switching off the UV lights after a particle growth stage, which stops the production of sulphuric acid and subsequently nucleation and growth. After sulphuric acid is reduced to background level, the exponential decay rate of the remaining particles in the chamber is measured (k_{tot}^{meas}, blue circles), which was not possible for the 1.8 nm channel due to low statistics. Decay of particles in the chamber is dominated by wall loss, dilution loss and coagulation loss to other particles. Particle loss rates are corrected for an averaged coagulation loss during the decay (k_{coag}^{avg}) to all particles larger than d_p and for the dilution loss (k_{dil}) (turquoise circles). They agree well with the expected wall loss rate $k_{wall}(d_p) = C_{wall} \cdot \sqrt{D_p(d_p)}$ (red dashed line) with $C_{wall} = 0.0077$ s$^{-0.5}$ cm^{-1} inferred from an independent sulphuric acid decay experiment in the absence of a particle sink, where the mobility diameter is assumed to be 0.82 nm (Ehrhart et al., 2016) (turquoise diamond). This suggests that there is negligible evaporation from the sulphuric acid particles above ca. 2 nm under the above mentioned experimental conditions, which would introduce another term disturbing the balance equation at each size. As all our growth-rate measurements, independent of the ammonia concentration and temperature, fall on the same line (see Fig. 1), this also points towards negligible evaporation effects at reduced ammonia levels (below 10 pptv) and up to 20°C.
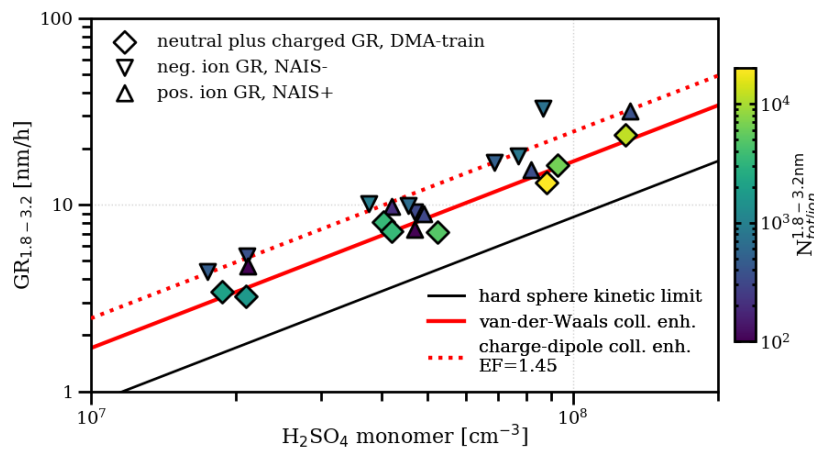
Figure 3: The effect of charge on growth. Measured growth rates of 1.8-3.2 nm (mobility diameter) particles and ions in experiments with ammonia above 25~~10~~ pptv. The DMA-train measures both neutral and charged particles (diamonds ~~with red contours~~) whereas the NAIS+/- (Manninen et al., 2009) measures purely charged particles (triangles ~~with blue contours~~). Both, the positively and negatively charged particle population have a faster apparent growth rate than the total particle population due to an enhanced collision rate from dipole-charge interactions. We measure a multiplicative charge enhancement factor of 1.45 in this size range with a combined fit to both polarities (~~blue~~ red ~~dashed~~ dotted line), which is consistent with estimates from average dipole orientation theory (Nadykto and Yu, 2003). At galactic cosmic rays ionization levels in the chamber, the charged fraction of the growing particles in the size-range 1.8-3.2 nm (mobility diameter) is between 5 and 25%. This is demonstrated by the colour code which indicates the integrated total or ion number concentration over the growth rate size interval averaged during the growth period. The fit of the appearance time for the total particle population is therefore affected on a minor level by the small earlier appearing charged fraction.
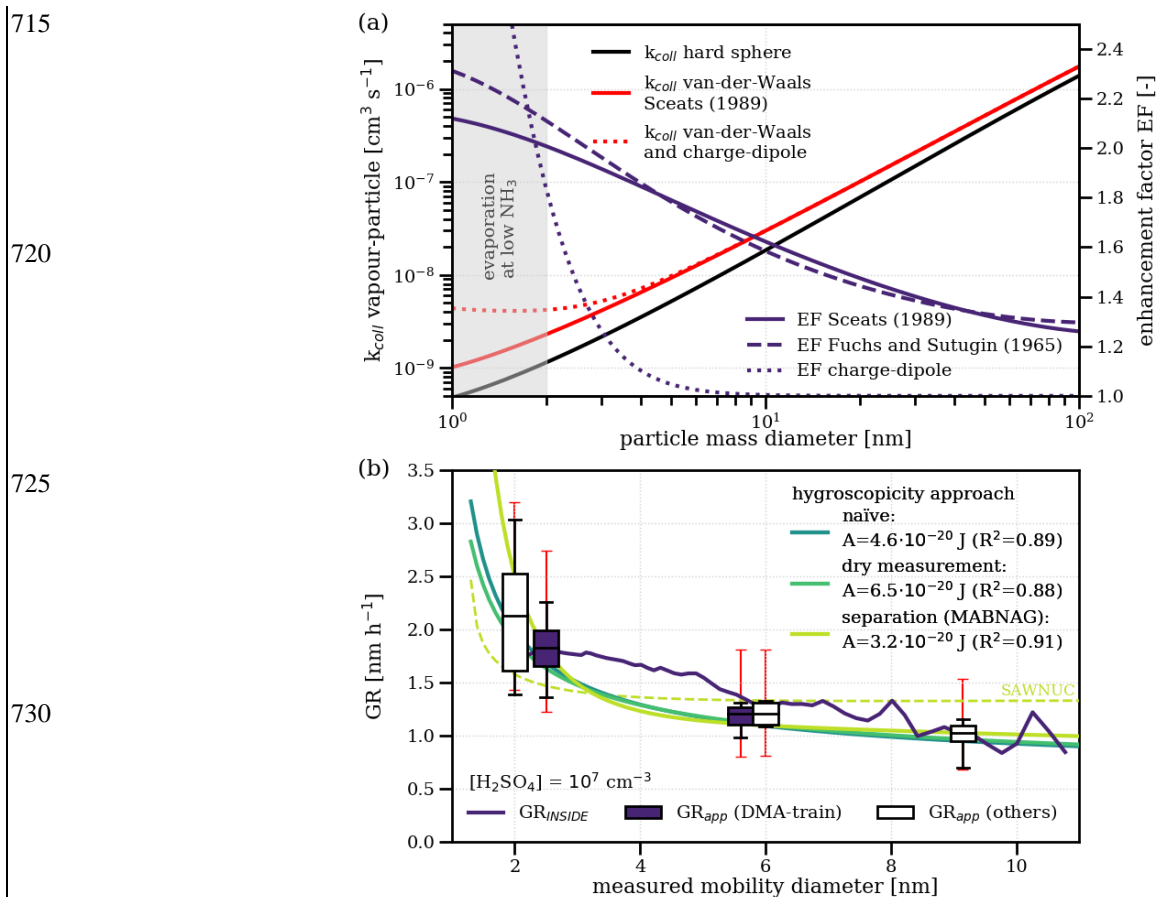
Figure 4: The size-dependency of sulphuric acid growth. ~~Measured and modelled size-dependency of growth rates.~~ (a) shows the theoretical collision rate of hydrated sulphuric acid vapour molecules $(m_v = M_{H2SO4} + 2M_{H2O})$ with particles of a certain mass diameter. The black line represents the hard-sphere limit, the red underline solid line also includes a collision enhancement due to van der Waals forces based on the approach of ($A = 4.6 \cdot 10^{-20}$ J), ~~while~~ and the red dashed line ~~is based~~ on the approach of ($A = 8.7 \cdot 10^{-20}$ J). The red dotted line additionally includes charge-dipole interactions based on average-dipole-orientation theory. The blue lines show the enhancement factor of a single attractive force ~~(charge-dipole interaction or van der Waals forces)~~ compared to the hard-sphere limit. (b) shows Tthe measured size-dependency of growth rates normalized to ~~Growth rates are normalized to~~ a sulphuric acid concentration of 10^7 cm^{-3}. ~~is shown in (b).~~ The solid blue line shows the growth rates inferred with the INSIDE method. ~~The growth rates were inferred with two different methods, the appearance time method (GR$_{app}$) and the INSIDE method (GR$_{INSIDE}$).~~ Filled boxes represent the appearance time growth rates from the DMA-train used to fit the Hamaker constant. Empty boxes represent appearance time growth rates from other instruments including the results from ~~(~~Lehtipalo et al.~~,~~ (2016) with high (>100 pptv) NH$_3$ concentrations. ~~Growth rates are normalized to a sulphuric acid concentration of 10^7 cm^{-3}.~~ For the appearance time growth-rate results, tThe ~~thick black line inside the~~ boxes ~~show~~ indicate the median and ~~of the results for a given size, the boxes indicate~~ the 50% interquartile range of the data, ~~while~~ and the whiskers represent the 90% quantile. The red small errorbars indicate the -33%/+50% systematic uncertainty in the sulphuric acid measurement. We show the size-dependency of three different approaches for particle hygroscopicity. The naïve approach (solid turquoise line), assuming the same hydration for vapour and particle; the dry measurement approach (solid light green line), assuming that the DMA-train measures completely dehydrated particles; and the separation approach (solid yellow line), assuming that available composition data from MABNAG can disentangle water uptake from sulphuric acid condensation. The separation approach using SAWNUC composition data is also shown as a dashed yellow line. ~~Also shown are the modelled growth rates for the geometric hard-sphere kinetic limit (solid black line) or the collision enhanced growth rates according to Eq. (S9) (solid and dashed red line). The grey shaded area includes the systematic uncertainty due to the assumed hydration of vapour and particles.~~
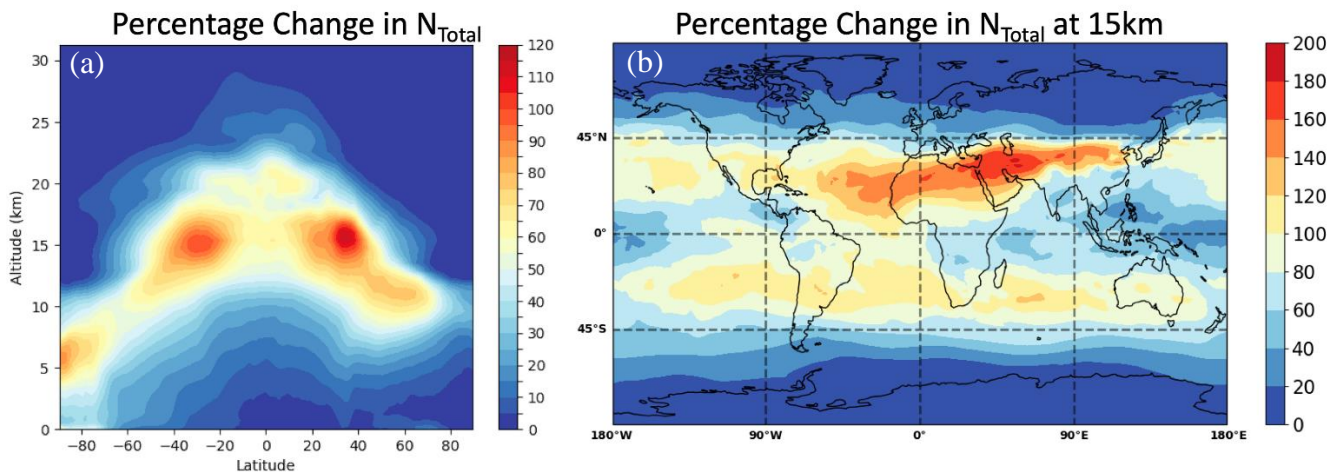
Figure 5: Increased global aerosol number concentrations due to the collision enhancement. Results from a global modeling study of the present-day atmosphere. (a) shows the relative change in total aerosol number concentration (particles larger 3 nm) averaged over all longitudes in a vertical profile if a collision enhancement is considered in sulphuric acid growth. (b) shows the relative increase at 15 km altitude on a global scale where the effects are most significant. Higher relative changes would be expected also at lower altitudes, if the model is adjusted for ternary sulphuric acid-water-ammonia nucleation.